

ISTANBUL TECHNICAL UNIVERSITY ★ GRADUATE SCHOOL

**FORMATION AND STRUCTURAL PROPERTIES OF WATER INDUCED
STRUCTURES AT GRAPHENE/MICA AND GRAPHENE/Cr_xO_y/GLASS
INTERFACES**



M.Sc. THESIS

Orkhan NOVRUZOV

Department of Nano Science and Nano Engineering

Nano Science and Nano Engineering Programme

OCTOBER 2021

ISTANBUL TECHNICAL UNIVERSITY ★ GRADUATE SCHOOL

**FORMATION AND STRUCTURAL PROPERTIES OF WATER INDUCED
STRUCTURES AT GRAPHENE/MICA AND GRAPHENE/Cr_xO_y/GLASS
INTERFACES**

M.Sc. THESIS

**Orkhan NOVRUZOV
(513171019)**

Department of Nano Science and Nano Engineering

Nano Science and Nano Engineering Programme

Thesis Advisor: Prof. Dr. Oğuzhan GÜRLÜ

OCTOBER 2021

İSTANBUL TEKNİK ÜNİVERSİTESİ ★ LİSANSÜSTÜ EĞİTİM ENSTİTÜSÜ

**GRAFEN/MİKA VE GRAFEN/Cr_xO_y/CAM ARAYÜZLERİNDE SU
KAYNAKLI YAPILARIN OLUŞUMU VE YAPISAL ÖZELLİKLERİNİN
İNCELENMESİ**

YÜKSEK LİSANS TEZİ

**Orkhan NOVRUZOV
(513171019)**

Nanobilim ve Nanomühendislik Anabilim Dalı

Nanobilim ve Nanomühendislik Programı

Tez Danışmanı: Prof. Dr. Oğuzhan GÜRLÜ

EKİM 2021

Orkhan NOVRUZOV, a M.Sc. student of İTÜ Graduate School student ID 513171019, successfully defended the thesis/dissertation entitled “FORMATION AND STRUCTURAL PROPERTIES OF WATER INDUCED STRUCTURES AT GRAPHENE/MICA AND GRAPHENE/Cr_xO_y/GLASS INTERFACES”, which he prepared after fulfilling the requirements specified in the associated legislations, before the jury whose signatures are below.

Thesis Advisor : **Prof. Dr. Oğuzhan GÜRLÜ**
Istanbul Technical University

Jury Members : **Dr. Nuri SOLAK**
Istanbul Technical University

Dr. Mustafa ARIKAN
TUBITAK ÜME University

Date of Submission : 04 October 2021
Date of Defense : 08 October 2021





To my family,



FOREWORD

“Try not to become a man of success. Rather become a man of value.”

Albert Einstaein

I would like to express my gratitude to a number of people who greatly assisted me in the process of my education and writing my master thesis.

Firts and foremost, I would like to thank my thesis advisor Prof. GÜRLÜ for his excellent support. It could not have been possible without his guidance and instructions.

I express my gratitude to Dr. Mustafa ARIKAN and Dr. Ayse Gokce OZBAY from TUBITAK UME.

My sincere thanks to NANOBEEs group members. I am profoundly grateful to Merve ERCELİK for her help.

I would like to thank my family for supporting and believing in me.

October 2021

Orkhan NOVRUZOV
(Engineer)



TABLE OF CONTENTS

	<u>Page</u>
FOREWORD	ix
TABLE OF CONTENTS	xi
ABBREVIATIONS	xiii
SYMBOLS	xv
LIST OF TABLES	xvii
LIST OF FIGURES	xix
SUMMARY	xxi
ÖZET	xxiii
1. INTRODUCTION	1
1.1 Purpose of Thesis	1
1.2 Literature Review	2
1.3 Hypothesis	3
2. EXPERIMENTAL	5
2.1 Optical Microscope	5
2.2 Scanning Probe Microscopy (SPM)	6
2.2.1 Atomic force microscopy	7
2.3 Profilometer	9
2.4 Physical Vapor Deposition(PVD)	9
2.4.1 Vacuum chamber	13
2.4.2 Evaporation boat	14
2.4.3 Quartz crystal microbalance (QMC)	14
3. SAMPLE PREPARATION AND EXPERIMENT	17
3.1 Thermal Evaporation of Chromium	17
3.2 Graphene Transferring	18
3.3 Annealing and Production of Cr _x O _y particles	19
3.4 Graphene/Mica	22
3.5 Water Interaction/Deposition on Cr _x O _y /Glass	22
4. RESULT AND DISCUSSION	25
4.1 Comparison of Fractal Formation Related to Deposited Thin Cr Film and Deposition Time	25
4.2 Water Interaction With Graphene/Cr _x O _y /Glass	28
4.3 Comparison of Surface Fractal formation on Graphene/Mica Samples	31
4.3.1 Rewetting in isolated box	31
4.3.2 Rewetting with graphene heater	32
5. CONCLUSIONS	33
REFERENCES	35
APPENDICES	37
CURRICULUM VITAE	43



ABBREVIATIONS

AFM	: Atomic Force Microscope
CVD	: Chemical Vapor Deposition
DI	: De-ionized
Gr	: Graphene
IPA	: Isopropyl alcohol
PMMA	: Poly(methyl methacrylate)
PVD	: Physical Vapor Deposition
QCM	: Quartz Crystal Microbalance
SPM	: Scanning Probe Microscopy/Microscopy
STM	: Scanning Tunneling Microscope
TMP	: Turbo Molecular Pump



SYMBOLS

A	: Ampere
Cr	: Chromium
Cr_xO_y	: Non-stoichiometric Chromium Oxide
d	: distance
f	: Frequency
NA	: Numerical Aperture
Si	: Silicon
Si₃N₄	: Silicon Nitride
SiO₂	: Silicon Dioxide
V	: Volt
α	: Angle
λ	: wavelenght



LIST OF TABLES

	<u>Page</u>
Table A.1 : Material table.	39
Table B.1 : QCM calibration table.	42





LIST OF FIGURES

	<u>Page</u>
Figure 1.1 : a)SPM image of fractal grown at $10\pm 1\%$ RH for 6 hours. b)Fractal growth illustration. c) Fractal growth area as a function of time. d) Drying overnight initiated formation finer and smaller fractals	2
Figure 1.2 : Image of water fractal from reflected light microscope	3
Figure 2.1 : Blurred two point by diffraction, the image of two point objects (red) can be resolved at distance d. Line profile from bottom shows the brightness along the direction of separation. Diagram taken from	5
Figure 2.2 : STM basic operation principle. Yellow spheres represent tip atoms and blue spheres represent array of sample atoms.	7
Figure 2.3 : Basic description of Atomic Force Microscope. 1) laser, 2) photodiode, 3) piezoelectric scanner, 4) cantilever, 5) sample surface.	8
Figure 2.4 : Curve representing tip-surface interaction and imaging mode. Pale Blue rectangle indicates dynamic mode, pale orange indicates intermittent contact mode and pale green indicates contact mode.	8
Figure 2.5 : Description of skidless stylus profilometer: 1) Tip, 2) Shaft(or beam), 3) Stylus movement(Z), 4) datum, 5) Measurement direction (X).	9
Figure 2.6 : Vapor Pressure curves of some Materials. Photo taken from	11
Figure 2.7 : The Distribution of deposited Atoms Vaporized from a Point Source and the thickness. Distribution of the Film Formed on a Planar Surface above the Source: Taken from	11
Figure 2.8 : Description of thermal deposition (evaporation). 1) Sensor (QCM), 2) vacuum pressure gauge, 3) copper evaporation legs, 4) evaporation boat.	12
Figure 2.9 : View of the vacuum chamber.	13
Figure 2.10 : Molybdenum boat clamp with copper and thermocouple put under it.	14
Figure 2.11 : Description of quartz crystal microbalance and working principle.	15
Figure 2.12 : Illustration of SQM160. a)QCM sensor and b)reference oscillator. ...	15
Figure 3.1 : $5\times 5\text{mm}^2$ substrates and mask. Yellow square indicates the position of the glass substrate.	17
Figure 3.2 : Shows chromium thin film on glass. Bright area that distinguished from rest is thin chromium film.	18
Figure 3.3 : Description of graphene/chromium/glass system.	19
Figure 3.4 : CVD furnace, A-tube furnace view, B-graph of heating rate and temperature stabilization.	20
Figure 3.5 : a)-Depicts $\text{Cr}_x\text{O}_y/\text{glass}$ after 450°C at $500\mu\text{m}$, b)-depicts inset of $\text{Cr}_x\text{O}_y/\text{Glass}$ at $20\mu\text{m}$, c)-shows $\text{Cr}_x\text{O}_y/\text{Glass}$ at $5\mu\text{m}$. Bright spots are chromium oxide nanoparticles.	21
Figure 3.6 : a-Grpahene/ $\text{Cr}_x\text{O}_y/\text{Glass}$ after annealing at 450°C at $500\mu\text{m}$. Inset from b-indicates graphene/ $\text{Cr}_x\text{O}_y/\text{glass}$ edge. Inset from c-indicates graphene/ $\text{Cr}_x\text{O}_y/\text{glass}$ from lower right.	21

Figure 3.7 : Basic illustration of graphene on mica. Pale yellow is mica substrate, blue one is intercalated water and black one over mica and water is graphene sheet.	22
Figure 3.8 : Optical microscope enclosed with stretch film and humidification unit. A-front view, B-side view, C-bubbler and flowmeter, D-nozzle.	23
Figure 4.1 : Pictures show chromium thin film sample that did not annealed homogeneously. a) shows sample with 500 μ m scale bar. b) Shows sample at 20 μ m scale bar. c) explain chromium thickness distribution on sample (green-chromium, blue-glass substrate).	25
Figure 4.2 : Indicated optic data was taken from exactly same location of the sample. Scale bar is 50 μ m. a is after thin film cr deposition, b after annealing at 450°C, c after first controlled humidification.	26
Figure 4.3 : Comparison of thin chromium film before and after annealing. a- after chromium deposition, b-after annealed at 500°C, c-after deposition, d-after annealed at 450°C.	27
Figure 4.4 : a and b give information about samples produced by Kivanc Esat a)chromium ultra thin filzm on glass and b) chromium oxides nano particles on glass. c and d our samples. c) after deposition of thin film chromium on glass and d) chromium oxide nanoparticles on glass.	27
Figure 4.5 : Illustartion chromium thin film on glass, a after deposition, b-after heat treatment at 450°C, c-during humidification, d-after humidifcation.	28
Figure 4.6 : Graphene/Cr _x O _y /Glass system.	29
Figure 4.7 : a-graphene/chromium oxide nano particle, b-fractal formed at non-graphene side of sample surface after humidification, c-fractal at chromium oxide nano particle graphene edge (red arrows in c indicate graphene frontier) d-inset indicate fractals at 100 μ m scale bar and e-indicate fractals at 20 μ m scale bar.	30
Figure 4.8 : a) graphene/CrxOy/glass at 500 μ m scale bar. b) red dotted enclosed lines shows graphene area, rest shows Cr _x O _y area, c) red dotted line indicates graphene covered area, rest area Cr _x O _y and glass.	31
Figure 4.9 : Graphene/Mica. A describes direct illumination Optic data, B describes back reflected illumination Optic data.	32
Figure A.1 : Front side and backside view of PVD system.	37
Figure A.2 : Connection order of vacuum gauge to power supply and multimeter.	38
Figure A.3 : SQM160 thickness monitor.	39
Figure A.4 : Evaporation unit power supply.	40
Figure A.5 : P&ID of PVD system. 1 vacuum chamber, 2 vacuum gauge, 3 Quartz Crystal Microbalance, 4 Evaporation unit and Mo boat, 5 power supply, 6 VAT (pneumatic) vale, 7 TMP, 8 Rotary positive displacement pump, 9 mist filter.	40
Figure B.1 : 13.5 nm thin film chromium on Si wafer. Red, green and black arrows indicates profilometer stylus movement direction.	41
Figure B.2 : 20.5 nm thin film chromium on Si wafer. Red and black arrows indicates profilometer stylus movement direction.	41
Figure B.3 : 23.9 nm thin film chromium on Si wafer. Red, green and black arrows indicates profilometer stylus movement direction.	42

FORMATION AND STRUCTURAL PROPERTIES OF WATER INDUCED STRUCTURES AT GRAPHENE/MICA AND GRAPHENE/Cr_xO_y/GLASS INTERFACES

SUMMARY

Water behavior at interfaces has great importance. Especially molecularly thin layer water or nanoconfined water. Nanoconfined water properties are different from bulk one. Studying nanoconfined water properties have fundamental importance in biology, material science, nanofluidics, tribology, and corrosion. Nanoconfinement materials are carbon nanotubes and layered two-dimensional materials or Van der Waals crystals.

In this thesis, we studied water interaction behavior with graphene/water/Cr_xO_y/glass and graphene/mica systems. For this purpose, we needed the following devices: Optic microscope with the isolated system, PVD system, graphene heater, and materials like CVD-grown graphene, muscovite mica, soda-lime glass, and chromium granulates.

Firstly, we started with graphene/water/Cr_xO_y/glass system. We did thermal evaporation of chromium using PVD system that was assembled in our laboratory. As a substrate, we used soda lime microscope slide glass (INTROLAB). Chromium thin-film on glass samples was produced. The thickness of thin-film chromium was varied. We transferred CVD-grown graphene onto chromium thin-film glass with the wet transfer method, then annealed it in a tube furnace around 450°C degrees under atmospheric ambient conditions for approximately 40 minutes. As soon as annealing finished we quickly transferred produced sample into a container full of silica gels to preserve from environmental humidity. We reduced humidity within enclosed boxes in which an Optical light microscope stayed for study samples under controlled humidification. We took optic data before, during, and after the humidification process.

Secondly, our second system for research was graphene/water/mica. Again as in the graphene/water/Cr_xO_y/glass system, we used CVD-grown graphene and V2grade muscovite mica (Ted Pella). Using scotch tape we cleavage mica several times then CVD-grown graphene was transferred onto it using the wet transfer method. We preserve graphene/mica samples in a container full of silica gels. We studied them with two methods: First under the optic microscope in the isolated box and second using the graphene heater. We reduced humidity to 9% in the isolated box using silica. In the case of the graphene heater, we managed to heat up nearly 200°C.

We observed fractal in graphene/Cr_xO_y/glass system but due to non-homogeneous deposition of chromium fractal formation was inconsistent. In case of graphene/mica system observation of de/wetting process was not possible even though we reduce humidity. The graphene heater was functional, the reason that we couldn't use it was a poorer resolution of the graphene/mica system. Otherwise, observation de/wetting graphene/water/mica with the optic microscope is challenging.



GRAFEN/MİKA VE GRAFEN/Cr_xO_y/CAM ARAYÜZEYLERİNDE SU KAYNAKLI YAPILARIN OLUŞUMU VE YAPISAL ÖZELLİKLERİNİN İNCELENMESİ

ÖZET

Ara yüzeydeki suyun davranışı büyük önem taşımaktadır. Özellikle moleküler ince tabakalı su ve ya nano-kapalı su. Nano-kapalı suyun özellikleri, üç boyutlu sudan farklıdır. Nano-kapalı su özelliklerinin incelenmesi, biyoloji, malzeme bilimi, nanoakışkanlar, triboloji ve korozyonda temel öneme sahiptir. Yüzeydeki molekül kalınlığında su tabakasının dış etkilere karşı çok hassa olmasından dolayı incelenmesi bir takım zorluklarla ilişkilidir. Yüzeydeki atom katmanı kalınlıktaki suyun probe mikroskop ile incelenmesi iki boyutlu malzemelerin keşfi ile daha detaylı incelendi. Özellikle grafenin keşfi bu görüntüleme işini kolaylaştırdı. İki boyutlu malzeme arasına sıkışmış nano kapalı su malzemenin elektronik yapısını değiştirme ve dope etme gibi özellikleri var. Nanokonfiment malzemeler karbon nanotüpler ve katmanlı iki boyutlu malzemeler veya katmanlı ve kolaylıkla kliv edilen van der Waals kristalları iki boyutlu malzemeler gibi geçiyor.

Bu tezde, grafen/Cr_xO_y/cam ve grafen/mika sistemleri ile su etkileşim davranışını inceledik. Bu amaçla sıraladığımız cihazlara ihtiyacımız var: İzole edilmiş sistemli optik mikroskop, PVD termal buharlaştırma sistemi, grafen ısıtıcı ve CVD ile büyütülmüş grafen, muskovit mika, sodyumlu camı ve krom granüller gibi malzemeler.

İlk olarak Cr_xO_y/cam ile başladık ve sonra grafen/Cr_xO_y/cam sistemi ile devam ettik. Krom iyi bir iletken olmasının yanı sıra geçiş metaldır ve cama iyi yapıştığı için ara katman yapıştırıcı gibi optik filtrelerin ve aktif matris dipeylerin üretiminde kullanılmaktadır. Bunun sebebi kromun oksitlenmesi ve cam matrisine difüzyon etmesidir. Öncelikle krom ince film camı inceledik ve nemlendirdikten sonra kuruma sürecinde gösterdiği özellikleri acaba grafen aktarıldıktan sonrada göstereceğini gözlemledik. Krom(Umicore) granülleri termal buharlaştırmasını laboratuvarımızda monte edilen PVD sistemi ile gerçekleştirdik. Alttaş olarak sodyumlu mikroskop camı(INTROLAB) kullandık. Değişik kalınlıklı krom ince filmler üretildi. Termal buharlaştırma cihazında örnekler dönmediyi için kaplama sonucunda elde ettiğimiz örneklerin yüzeyinde kromun dağılımı homojen olmamıştır. İnce film krom kalınlıkları çeşitlendirildi. Cam yüzeylere krom kaplamadan önce camlar 5mm x 5mm ölçülerde elmasla kesildi ve referans noktaları yapıldı. Genel olarak her kaplama sürecinde genel olarak 5 adet cam kullandık. Sonra kimyasal temizleme yöntemi ile aseton, izopropil alkol, metil alkol ve de-ionize edilmiş su ile her biri 5 dakika olmakla ultrasonik banyoda temizlendi. Temizlenmiş örnekler azot tabancası ile kurutuldu. Kurutulmuş örnekler plazma temizleyiciye, DIENER-e konuldu ve 5 dakika Argon ve Oksijen gaz karışımı ile temizlendi. Plazma temizleme parametreleri argonun akış hızı 45 standart kubik santimetre, oksijenin için akış hızı 5 standart kubik santimetre, güç 20% oranla 50 W. Temizlenmiş örnekler maskelendi ve kapton bantla maskeye ve döner çemberin diskine yapıştırıldı ve krom ince film kaplandı. Önceden CVD

prosesle büyütülmüş grafen uygun boyutta kesildi ve örnek üzerine transfer etmek için hazırlandı. Bundan sonra CVD ile büyütülen grafeni krom ince film cam üzerine ıslak transfer yöntemiyle aktardık. Grafen/Krom/Cam örneği optik mikroskopda incelendi. Optik mikroskopda incelendikten sonra tüp fırında atmosferik ortamda 450°C derece sıcaklığında yaklaşık 40 dakika fırınladık.

Örnekleri çevredeki nemden mühafıza etmek için silika jelli kutularda sakladık. İncelenen numuneler için Optik mikroskopunun civarını metal iskeleden çerçeve yaptık ve streç filmle civarını sardık. Optik mikroskopun bulunduğu kutuda nemi silika jellerin yardımı ile düşürdük. Kutudaki nem ortamını kontrollu tutmak için silika jelleri bir süre sonra yeniledik. Nemlendirme işlemi öncesi, nemlendirme sırasında ve nemlendirmeden sonrasında k1 optik verileri aldık.

İkinci olarak, araştırma için ikinci sistemimiz grafen/mika sistemidir. Yine grafen/Cr_xO_y/cam sisteminde olduğu gibi CVD yöntemi ile büyütülen grafen ve V2 dereceli muskovit mika (Ted Pella) kullandık. Mika altlık kısmında kullanarak CVD yöntemi ile büyütülmüş grafeni üzerine ıslak transfer yöntemi ile aktardık. Grafen/mika numunelerini silika jellerle dolu bir kapta mühafıza etdik. Örnekleri iki yöntemle inceledik: birinci yöntemde izole edilmiş kutuda optik mikroskopun kullanarak inceledik ve ikinci yöntemle grafen ısıtıcı kullanarak. İzole edilmiş kutuda nemi siliki jel ile %9'a indirdik. Düşük nemlikte örneği 12 saat kutuda beklettik fakat herhangi bir değişiklik gözlenmedi. Nem kutusuna azot tüpünden düşük basınçta azot üfledik. Kutudaki nemlik 4.5% kadar indi lakin uzun süre düşük nemlilikte tutamadık. (tüp hacmine bağlı olarak) Grafen ısıtıcı sıcaklığı yaklaşık 200°C'ye kadar ısıtmayı başardık. Buna rağmen grafen/mika örneğinde nemsizleşmeden dolayı fraktal oluşumunu gözlemleyemedik.

Cr_xO_y/cam ile yaptığımız araştırma sonucunda tüm yüzeyde su kaynaklı fraktal oluşumu bölgesel olarak gözlemledik. Suyun fraktal şekilli dallanmasına sebep krom ince film kaplı yüzeyde defektlerin olmasıdır. Bu defektler suyun fraktal şeklinde dallanması için çekirdek rolünü oynamıştır. Oluşan fraktalların dalları ince olmakla yanı sıra diğere fraktalların dalları ile örtüşmüyor. Termal buharlaştırma yöntemi ile kapladığımız örneklerin yüzeyine krom ince film homojen olarak kaplanmamış. Bunun nedeni PVD sistemimizdeki döndürücü motorun olmamasından dolayı örneklerin dönmemesidir. Bir önceki araştırmadaki prosedür ile yapılmış örneklerle bizim yaptığımız örnekleri kıyasladık ve bazı benzerlikler ve farklılıklar gözlemledik. Bizim yaptığımız örneklerde krom ince film 450°C toplam 37-40 dakikaya kadar fırınladık ve krom oksid nano parçacıkları gözlemledik. Bu oksid nano parçacıklar noktasal olarak kaplanan yüzeyde homojen olmayan şekilde dağılmıştır.

Grafen/Cr_xO_y/cam sisteminde fraktal gözlemledik ancak kromun yüzeyde homojen olmayan birikiminden dolayı fraktal oluşumu tüm yüzeyde bölgesel olarak gözlemledik. Su ile grafen/Cr_xO_y/cam yüzeyinin etkileşiminden fraktal yapılar Cr_xO_y/cam, grafen/Cr_xO_y/cam sınırında ve tamamen grafenli bölgelerde de gözlemledik. Grafenli bölgelerde oluşan fraktal yapılar çiçek şeklinde olup Cr_xO_y yüzeyindeki fraktallarla karşılaştırdıkta daha az dallanmıştır.

Grafen/mika örneğini %9 nemlilikte izole kutusunda toplam 12 saatten fazla sürede düşük nemde beklettik. Grafen/mika sisteminde nemi düşürmemize rağmen tekrar ıslatma gözlemlenmesi mümkün olmadı. Grafen ısıtıcı kullanarak Grafen/mika örneğinde fraktal yapı oluşumuna termal etkiyi denedik. Grafen ısıtıcı kullanmamıza rağmen grafen/mika sistemindeki çözünürlüğün düşük olmasından dolayı, optik

mikroskop ile grafen/mika örneğinin nemsizleşmeden dolayı fraktal oluşumunu gözlemleyemedik.





1. INTRODUCTION

Behaviour of substances at the interface differs from the bulk one. The interaction of the first layer of water with substance has great importance in biology, material science, electrochemistry and corrosion. We studied water structure at interface of layered materials.

1.1 Purpose of Thesis

In this thesis, we studied both water intercalation at Graphene/Cr_xO_y/Glass and Graphene/Mica interfaces. Water at interfaces of two-dimensional material has properties that induce doping. Moreover, the frictional properties of materials are greatly changed. We deposited thin film chromium onto soda-lime glass with varying thicknesses and annealed it at 450°C for approximately 40 minutes. Annealing Chromium/Glass results in the formation of Chromium oxide nanoparticles. Under humidity-controlled set up we contaminated Chromium oxide/glass sample with water and observed partial fractal formations over the sample surface. In addition, CVD-grown graphene was transferred onto newly chromium deposited soda-lime glass and annealed at 450°C for nearly 40 minutes. The partial fractal formation was observed at Graphene/Cr_xO_y/glass as at Cr_xO_y/Glass interface. We made attempted to observe water intercalation at Graphene/mica interface using an optical microscope by two methods: The first method in reduced humidity box and the second method heating with graphene heater to 180°C. Unfortunately, neither the first method nor the second method gave results. Fractal formations were not observed in both methods for graphene/mica samples. We realized that the chromium oxides nanoparticle formed after annealing of ultra thin-film chromium on glass and if the thickness of it exceeds definite thickness oxide nanoparticle islands connect together to form a smooth surface and as a result fractal formation does not occur. In this thesis, we studied graphene/CrxOy/glass system with varying thickness of chromium response to the controlled humidification with DI water.

1.2 Literature Review

Study thin layer water structure with an optical microscope is rather difficult. Despite AFM advancement it still has some problems in imaging water-thin layer on surfaces because of tip perturbation of molecular thin layer water. Water on mica surface was studied using scanning polarization force microscopy [5]. The drawback of Scanning Polarization Force Microscopy is poor lateral resolution. The advent of graphene material made it possible to study dynamic properties of the molecularly thin layer of water. The wetting/dewetting process occurs, when the relative humidity is manipulated [1,6].

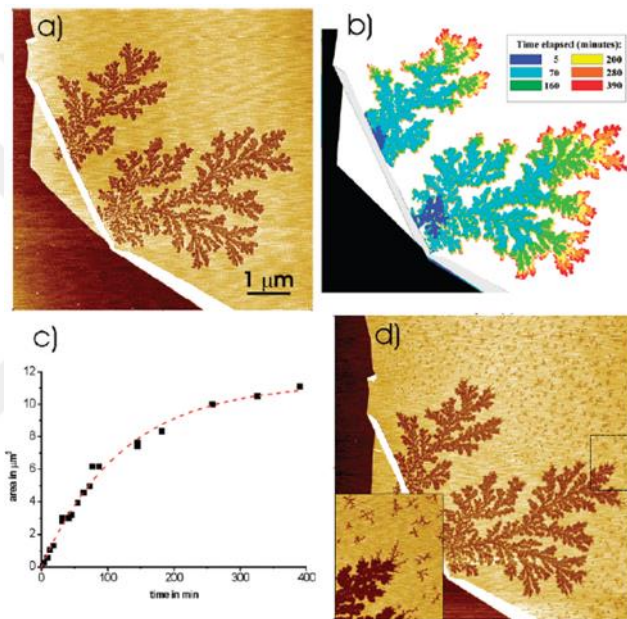


Figure 1.1 : a)SPM image of fractal grown at $10\pm 1\%$ RH for 6 hours. b)Fractal growth illustration. c) Fractal growth area as a function of time. d) Drying overnight initiated formation finer and smaller fractals [1].

Thermal processing graphene/mica system results in the removal of intercalated water [7,8]. Water at interfaces within two-dimensional materials shows different properties rather than bulk ones. Moreover, nanoconfined water changes the electronic and frictional properties of materials. Direct imaging water layer at subnanometric range using an optical microscope is challenging. Water intercalation in graphene/mica system is observed using SPM [9–11]. As humidity reduces fractal formation occurs, as well as the humidity increases, when fractal formation disappears. The fractal formation is a function of relative humidity.

Chromium is a transition metal. Besides good conductivity, it has excellent adhesion properties to the soda-lime glass. Better adhesion related to graded metal oxide formation with glass matrix [12,13]. Kivanc Esat observed fractal formation humidifying in a controlled manner annealed thin-film chromium glass [2].



Figure 1.2 : Image of water fractal from reflected light microscope [2].

1.3 Hypothesis

Humidifying ultra-thin layer of chromium oxide with water results in forming fractal structures. Increasing thickness of chromium thickness will have an adverse tendency in forming and propagation fractals. Kivanc Esat named Fractal morphology of water on chromium oxide thin films that observed fractal formation in his master thesis [2]. We repeated it with chromium oxide thin film and observed partly fractal formation. If we do it with graphene/chromium oxide thin film/glass after drying fractal formation should be observed from defects of the surface. Annealing process initiates defects formation on graphene and that defects will be the nucleation point of fractal formation.



2. EXPERIMENTAL

2.1 Optical Microscope

The invention of compound light microscope in sixteenth century gave opportunities to scientist to inspect matter and biological specimens. Since the microscopes invention and its ability about studying small features of the sample with scrutiny rose dramatically. The basic operation principle can be described using ray optics. However, when sizes are to be studied of the order of the wavelength of visible light, i.e. 400–800 nm, we have to take into account the wave properties of light such as interference and diffraction. It is impossible to achieve high resolution simply by increasing magnification of the lens arrangement [14]. Figure 2.1 explains

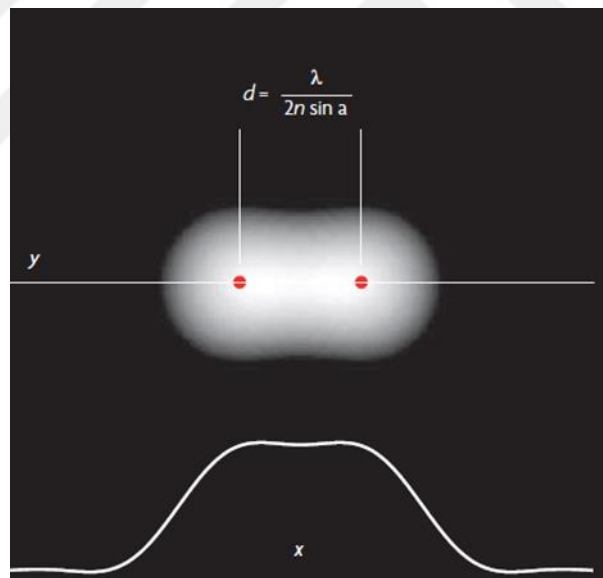


Figure 2.1 : Blurred two point by diffraction, the image of two point objects (red) can be resolved at distance d . Line profile from bottom shows the brightness along the direction of separation. Diagram taken from [3].

Ernst Abbe demonstrated how this diffraction-limited resolution can be enhanced if the illumination directed at an angle with respect to the optical axis. In this case, the diffraction limit is determined by the sum of the numerical apertures of the illumination lens and the collection lens.

If the angles of incidence and collection are identical, a factor of 2 is obtained, leading to the famous Abbe formula [3,14]

$$d = \frac{\lambda}{2NA}, NA=n*\sin\alpha \quad (2.1)$$

d-distance between two point, λ -wavelength, NA-Numerical Aperture, $n*\sin\alpha$ -angle of the cone focused light

Abbe's formula can be used as a general criterion for resolving its spatial features [14].

We used an Olympus BX51 optic microscope which has digital camera DP 25 to examine samples. Physical ability of Olympus BX51 is 1000x magnification.

2.2 Scanning Probe Microscopy (SPM)

Scanning probe microscopy is a critical technique in the rapidly developing nanoscience field. SPM range of imaging is from several 100 μ m to 10 pm. SPM makes it possible to image surfaces with atomic resolution. Moreover, it gives information about structural defects like step edges, point defects, and adsorbates. The basic underlying concept of SPM relies on the interaction between a probe and investigated surface.

The geometrical shape of the probe affects resolution. Simply Probe is a tip with a conical shape. If the surface step edge is steeper then the opening angle of the cone image will be with smeared contour. By contrast, if a hole on the surface of the sample is smaller than the apex diameter of a probe image of the hole will not be imaged or will be appeared with distortion. Using SPM gives us the following opportunities: Firstly, reveals the topography of the sample surface (one should not perceive it as a geometrical topography). Secondly, it gives an opportunity to the local measurement of the surface, in the case of Scanning Tunneling Microscope (STM) using spectroscopic modes we can get information about the electronic structure of the sample surface and Scanning Force Microscope (SFM) allows to determine electrostatic forces. Thirdly, Utilizing SPM manipulation with atoms or molecules is possible [15]. Firstly, Scanning Tunneling Microscope (STM) was invented by Binnig and Rohrer in 1982. Figure 2.2 describes main operation principle of the STM.

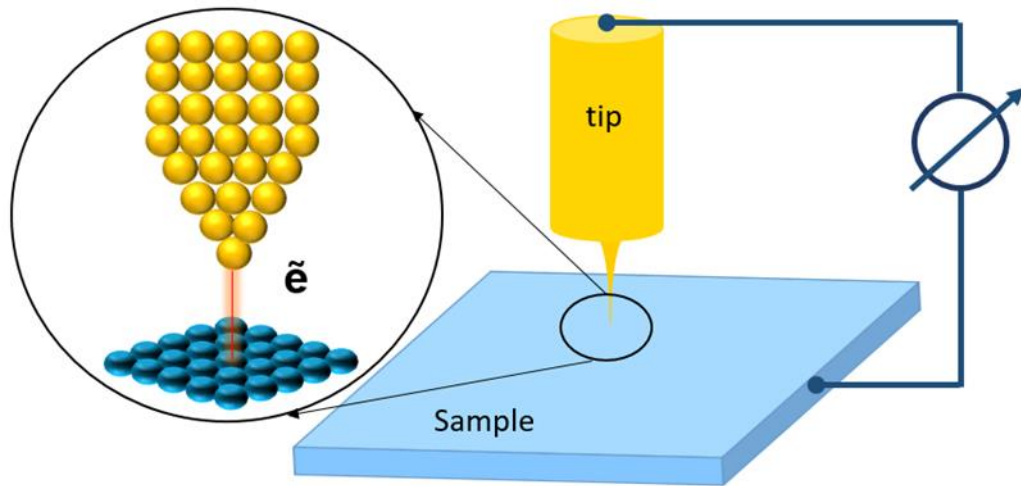


Figure 2.2 : STM basic operation principle. Yellow spheres represent tip atoms and blue spheres represent array of sample atoms.

STM basic operation principle is based on quantum mechanical phenomena also known as tunneling. It consists of the sharp tip usually made from W and Pt-Ir alloy, coarse approach mechanism, piezoelectric-driven stick-slip motore, dedicated electronics and computer. Probe tip brought few Angstrom distances with sample as the wavefunction of tip and sample overlap. In few Angstrom distances electron tunneled through vacuum gap. STM gives information about density of states of sample. The drawback of STM is that it can be applied only in conductive materials. Studying dielectric with STM impossible [16,17].

2.2.1 Atomic force microscopy

The main concept of force techniques is measuring the force between sharp tip and surface. Sharp tip is mounted on a lever that called as cantilever. Cantilever acts as a force sensor. Cantilevers are usually made from Si, SiO₂, Si₃N₄ and two shapes of cantilever are predominant: triangular and rectangular. Minute changes of cantilever have to be detected. There are several methods invented to detect tiny deflection of the cantilever. The most common and practical one is beam deflection method. Feedback mechanism maintains cantilever in pre-set value and monitor piezoelectric and amplifier is main part of feedback mechanism. It operates as follow: laser beam shines on the rear side of the cantilever and deflects on to a 4 quadrant photodiode. Four segmented photodiode convert laser deflected from cantilever into according signal and displays on computer. AFM operates either in contact mode or dynamic mode. Moreover, AFM gives us opportunity to do force measurement, topographic imaging and manipulation. In contact mode, the cantilever contacts with the surface.

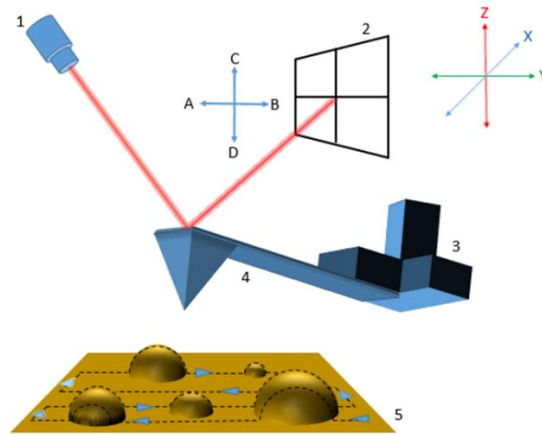


Figure 2.3 : Basic description of Atomic Force Microscope. 1) laser, 2) photodiode, 3) piezoelectric scanner, 4) cantilever, 5) sample surface.

On the contrary, dynamic mode operates at some height from sample surface and detect topography of the surface as the dynamic properties of cantilever changes. In this mode it does not damage the sample surface due to non-physical contact [15,18,19].

In figure 2.4 essential features of tip-sample interaction and imaging modes are illustrated. Force distance curve describes tip sample interaction nature and in each position respective operation mode. In pale blue region dynamic mode is predominant as cantilever approaches futher to sample region with pale green indicated contact mode. Region between contact and dynamic mode depicts intermittent contact mode. Furthermore, intermittent contact mode or tapping mode cantilever vibrates and intermittently touches the sample surface.

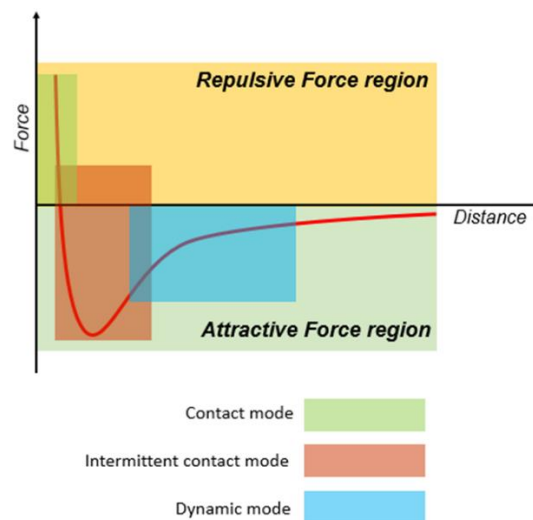


Figure 2.4 : Curve representing tip-surface interaction and imaging mode. Pale Blue rectangle indicates dynamic mode, pale orange indicates intermittent contact mode and pale green indicates contact mode.

2.3 Profilometer

Determination of uppermost surface has a crucial importance. Uppermost part of the surface has series of valley and peaks of different height, depth and spacing. Surface profiler or profilometer is an effective instrument in order to measure surface texture. Generally profilometer is divided into two groups: Contact profilometer and optical profilometer (non-contact profilometer). Among numerous metrology ability stylus profilometer can measure height with nanometer precision. Stylus profilometer main components are stylus, gauge and data acquisition system. Tip is attached at the end of stylus and is usually made from wear resistant material as diamond or sapphire being in a conical shape. In figure 2.5 skidless stylus profilometer are illustrated. Measurement is made as follows through precise control of load stylus slightly dragged along the surface. The stylus tip moves in a line moving tip vertically over peaks and valleys. Variation in stylus position is registered electrically and created in profile. Measured profile is height variation of stylus against horizontal axis [20,21].

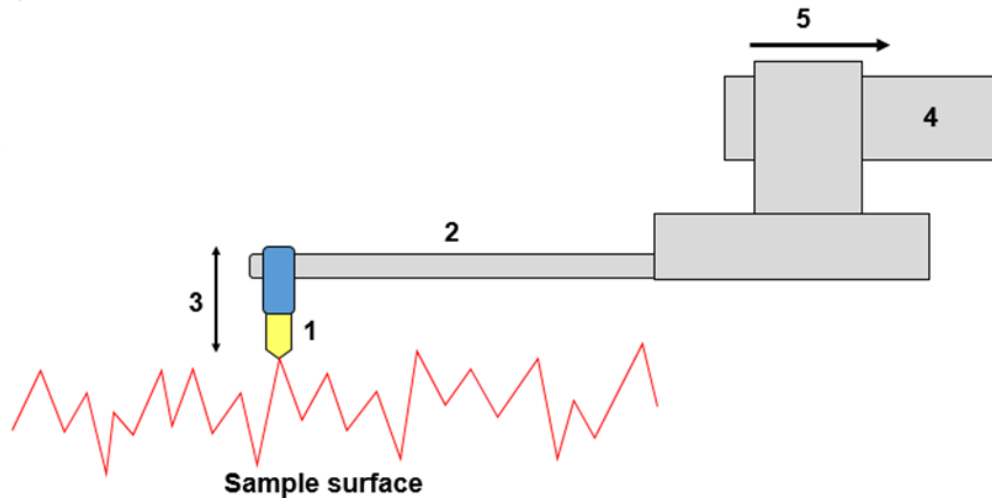


Figure 2.5 : Description of skidless stylus profilometer: 1) Tip, 2) Shaft(or beam), 3) Stylus movement(Z), 4) datum, 5) Measurement direction (X).

2.4 Physical Vapor Deposition(PVD)

Surface engineering deals with studying and modification/changing surface or near surface region of the materials in desired way. This can be achieved most commonly in two ways: Surface modification and overlay processes. Overlay process is adding new material layers to the substrate in such way that substrate couldn't detect. Surface modification process is the modification of the surface of the substrate without adding any chemical materials. One of the overlay adding method is Physical Vapor

Deposition (PVD). PVD is an atomistic deposition technique that vaporized atom and molecule from a solid or from a liquid source and as a vapor of atoms or molecules delivered to the substrate under low pressure environment. Generally, a film less than 1 μm thickness is referred as a thin film. Thicker films are called coatings. Main types of PVD are the following: vacuum evaporation, sputter deposition, arc vapor deposition, ion plating and so on. Application range of vacuum deposition is wide and it covers optical interference coating till electrically conducting film deposition.

This paper heavily relies on vacuum deposition (evaporation). Underlying the principle of vacuum deposition/evaporation is that atoms and molecules from thermally vaporizing source (material) transport to the substrate surface and condense without collision or with negligible collision with residual gas in the vacuum chamber. For vacuum evaporation vacuum have to be better than 10^{-4} mbar. Such a low pressure increases mean free path between collisions. In our case vacuum is in range of 1.3×10^{-6} mbar. For minimal deposition on substrate vapor pressure of evaporated materials should be nearly 10^{-2} mbar. If at indicated pressure value evaporated material is solid, the process is called sublimation. On the contrary, if at indicated value evaporated material is in molten condition then process is called evaporation. Figure 2.6 describes some elements equilibrium vapor pressure as a function of temperature.

Some elements evaporate and some elements such as chromium (Cr), cadmium (Cd), magnesium (Mg), arsenic (As) and carbon(C) sublime. For instance, it is shown in figure 2.5, vapor pressure of chromium 10^{-2} Torr corresponds to 600°C which is below melting point. For this reason chromium is vaporized by sublimating. In case of materials such as aluminum (Al), tin (Sn), gallium (Ga) and lead (Pb) which have low vapor pressure above molten condition. For example Al and Pb have 10^{-2} torr vapor pressure about 500°C higher above their melting point. For detail refer to figure 2.6.

At low evaporation rate, deposition flux distribution is obey cosine distribution. In figure 2.7 showed distribution of material on the substrate evaporated from the point source.

Θ is the angle from the normal to the vaporizing surface

ϕ is the angle from a line from the source to a point on the substrate

dm/dA is mass per unit area

r is distance from source to the substrate

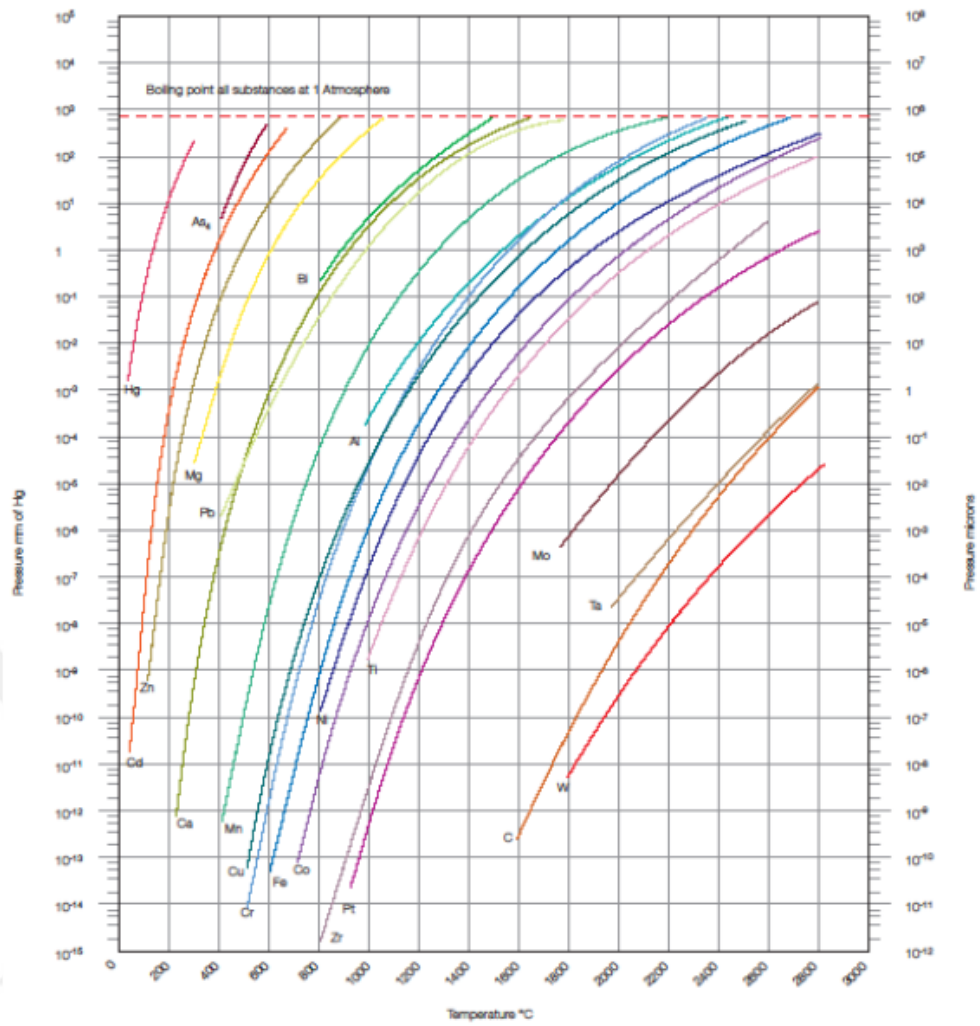
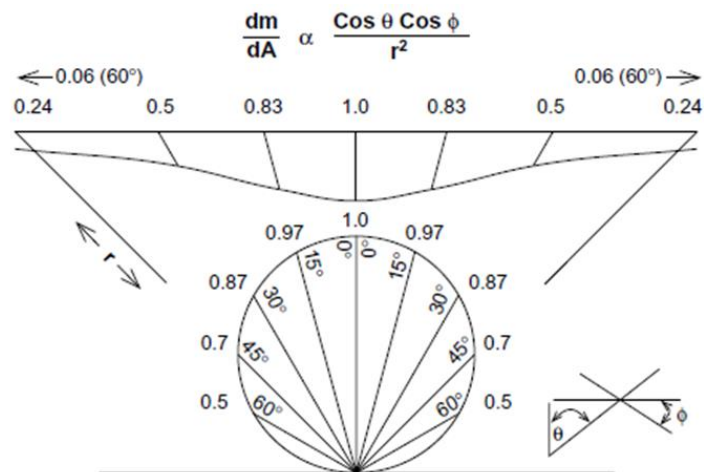


Figure 2.6 : Vapor Pressure curves of some Materials. Photo taken from [4].



Cosine distribution

Top, relative deposition on a planar surface from a point source of vaporization
Bottom, relative vaporization as a function of angle from normal

Figure 2.7 : The Distribution of deposited Atoms Vaporized from a Point Source and the thickness. Distribution of the Film Formed on a Planar Surface above the Source: Taken from [22].

PVD system assembled in our laboratory has following components:

- Vacuum Chamber
- Mechanical oil sealed pump (Edwards28M),
- Turbo Molecular Pump(SHIMADZU TMP 803LM),
- VAT valve,
- Inficon cold cathode gauge mpg-500,
- Thickness monitor, inficon sqm-160,
- evaporation unit,
- cooling system,
- power supply TDK-lambda for evaporation unit,
- molybdenum boat

Mechanical pump reduces the pressure to 10^{-3} mbar during 20-30 minutes. Exhaust system has one oil filter and one mist filter. Figure 2.8 illustrates basic principle of the PVD system.

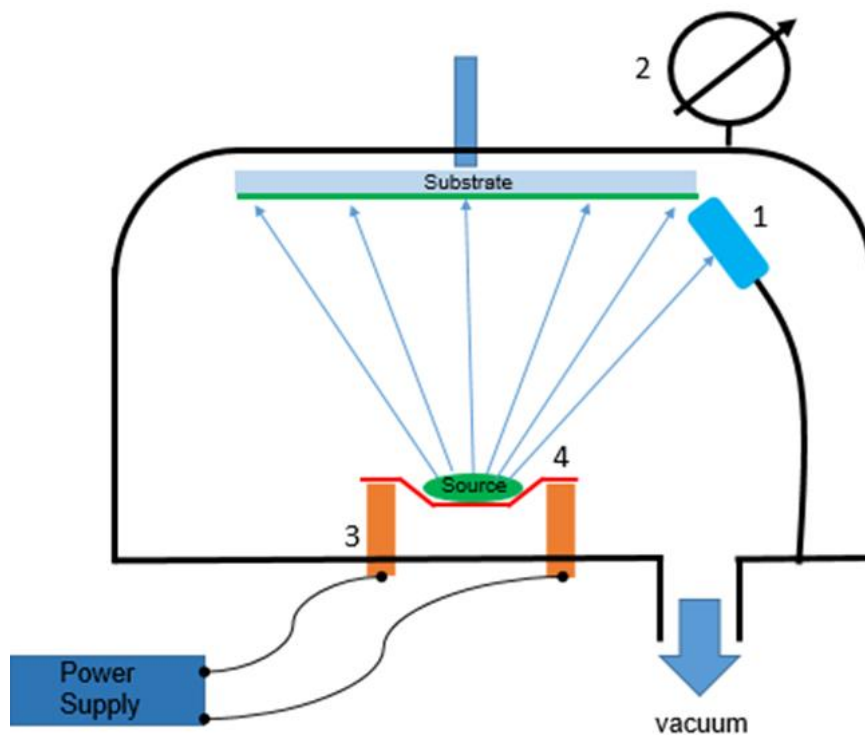


Figure 2.8 : Description of thermal deposition (evaporation). 1) Sensor (QCM), 2) vacuum pressure gauge, 3) copper evaporation legs, 4) evaporation boat.

Using TMP we can reduce pressure within vacuum chamber 10⁻⁶ mbar. The pressure should be between 4-7 bar. At closed position, it mechanically locked. Inside chamber inficon mpg500 pressure gauge were used. QCM is used to monitor deposition rate and thickness of the deposited material.

2.4.1 Vacuum chamber

Vacuum chamber in our case is direct load chamber, which it's internal dimension is 57x54x50cm and is made from stainless steel(304). Volume of vacuum chamber is approximately 153.9 dm³(lt). The distance between boat and fixture is 15 cm. Tooling has four circular places for fixtures whose diameters are 12.6cm. Figure 2.9 shows front view of vacuum chamber.

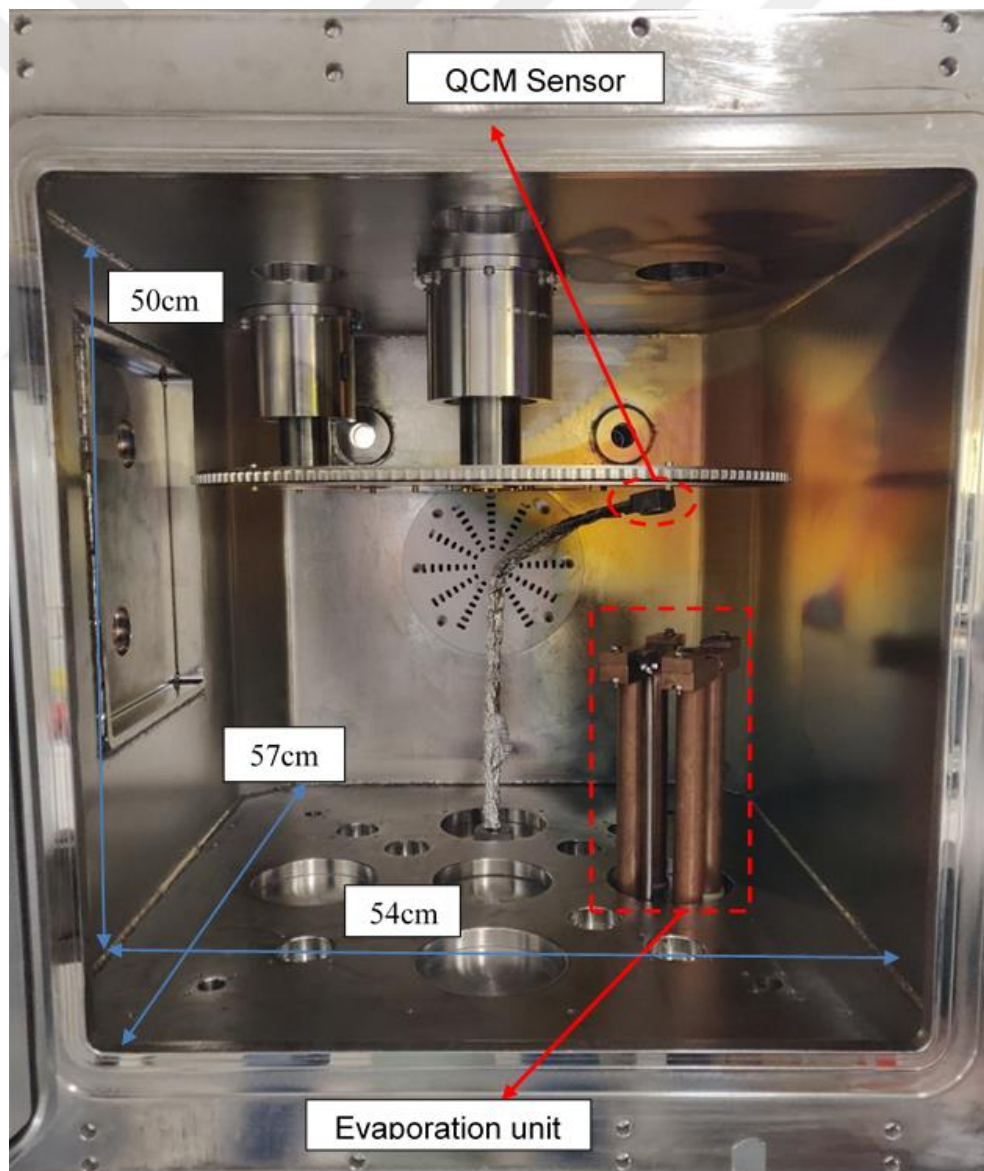


Figure 2.9 : View of the vacuum chamber.

2.4.2 Evaporation boat

The evaporation boat is commonly made from refractory metals such as W, Ta, and Mo. We shaped the evaporation boat from thin sheet of molybdenum. Before using molybdenum (Mo), we made it from tungsten (W) sheet, however unfortunately, due to brittleness of tungsten, we failed and during shaping, it cracked and we decided to use molybdenum (Mo). Figure 2.10 shows molybdenum boat that is used in chromium and copper evaporation.

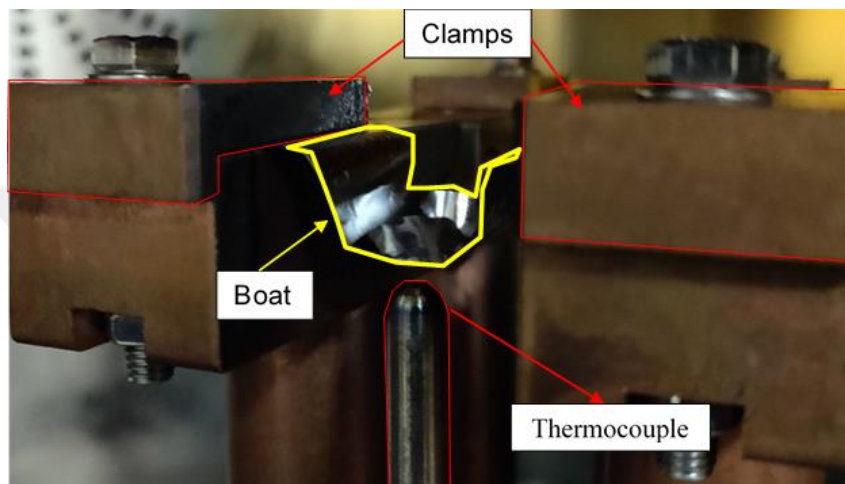


Figure 2.10 : Molybdenum boat clamp with copper and thermocouple put under it.

Thermocouple is located directly under molybdenum boat.

2.4.3 Quartz crystal microbalance (QMC)

Thickness monitor is indispensable component in PVD techniques. It measures thickness, mass and deposition rate of source that deposits on substrate. Measurement process takes place in situ. With proper calibration, this tool gives a chance to control the deposition rate, thickness and mass. The most essential component of thickness monitor is QCM sensor. Quartz crystal is piezoelectric material which reacts to voltage with mechanical changing of its shape. AT-cut quartz crystal oscillates when voltage is applied and oscillates at fixed frequency. During this oscillation, deposited material accumulates on the surface of crystal thus reducing frequency. Reduction in frequency is proportional with added mass. Reaction quartz the crystal to the lowest frequency and generally a thickness shear mode is fundamental. The thickness shear mode distinctive movement is parallel to the main monitor crystal. The feedback of the quartz crystal at higher frequency called anharmonics. Anharmonics are mixture of the thickness shear and thickness twist modes. The design of monitor crystal is illustrated

in figure 2.11. Blue region indicates AT cut quartz crystal and yellow contouring region shows gold coating. Red dotted line describes shear modes.

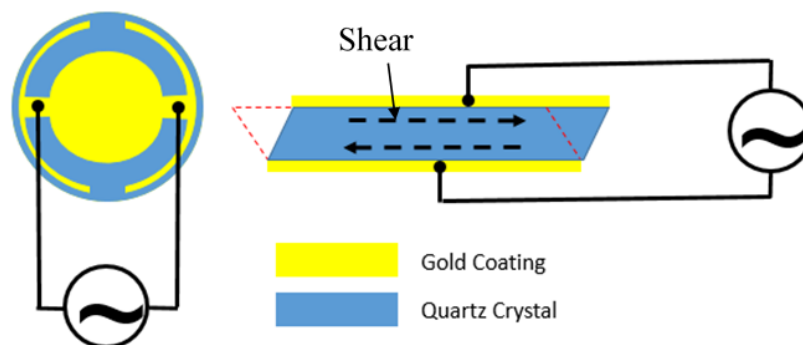


Figure 2.11 : Description of quartz crystal microbalance and working principle.

Circular QCM is the result of several refinements and these improvements are the followings: First one was with circular shape symmetry that leads to significantly reducing vibrational mode. Second was contour one the face of the crystal to cut down the size of the exciting electrode. As a result of this refinement were trapping the acoustic energy. Excitation is limited to the core area when the electrode diameter is reduced [23–26].

We use Inficon SQM160 rate/thickness monitor to measure the thickness of deposited materials. Starting oscillation frequency of QCM was 5.98 MHz. Photos in figure 2.12 shows SQM160 sensor and reference oscillator. In vac cable coated with aluminum foil to preserve from deposited materials.

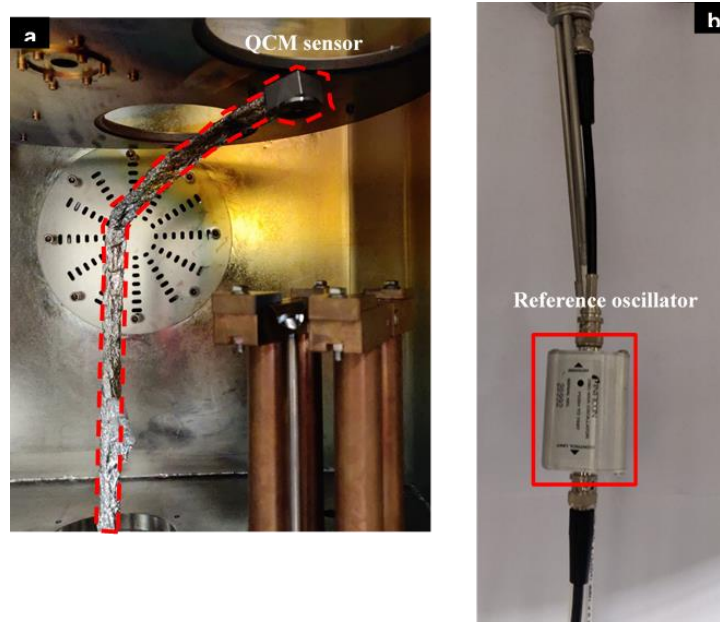


Figure 2.12 : Illustration of SQM160. a)QCM sensor and b)reference oscillator.



3. SAMPLE PREPARATION AND EXPERIMENT

3.1 Thermal Evaporation of Chromium

We produced samples utilizing PVD system. Before thermal deposition, substrates underwent a cleaning procedure. As a substrate, we used INTROLAB soda-lime microscope slide glass. Figure 3.1 describes the glass substrates and mask.

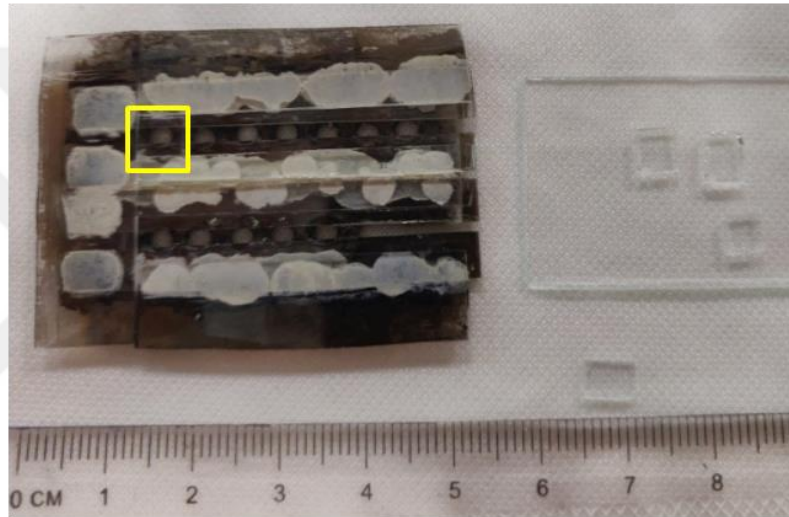


Figure 3.1 : 5x5mm² substrates and mask. Yellow square indicates the position of the glass substrate.

We cut from microscope slide by dimension 5mm x5mm glass substrates. All newly cut glass substrates were marked with the reference mark that was the same side of the frosted edge of the microscope slide. Hand grinder was handy in shaping glass substrates. As soon as glass substrates were ready, they went through chemical treatment. Chemical treatment happened in ultrasonic bath and with the following chemical reagents Acetone, IPA, Methanol and DI water each respectively for 5 minutes. After chemical cleaning, we blew it with nitrogen in order to dry it. Afterwards, glass substrates were cleaned with plasma etching (Diener) for 5 minutes with oxygen and argon gas mixture for 5 minutes. Parameters were the following: O₂ 5sccm, Ar 45sccm, voltage 157V, 20% of total power, fluctuation of current between 330mA and 340mA. Glass mask with 3mm hole diameter was wiped with acetone using Q-tips and dry using nitrogen.

At the end of the cleaning procedure, substrates were cleaned and they were ready to fit into the mask and fixed to the desired position. For this purpose, we used Kapton tape (polyimide), as it is vacuum compatible. We located the mask directly under the evaporation boat, where “Umicore” chromium granules were used. The evaporation process started when the pressure decreased to 10^{-6} mbar. Pressure monitored with cold cathode gauge INFICON (mpg500) that the range is 1000mbar- 10^{-9} mbar. Approximately 95A and 2.7V applied to copper rods. Copper rods of the evaporation unit QCM sensor are cooled with water and during 95A current flow boat is heated. Heated boat triggered sublimation of chromium granules, so we could observe glowing from view port of PVD system that indicates deposition has started. Figure 3.2 shows a sample after thermal evaporation. Bright area indicates thin-film chromium.

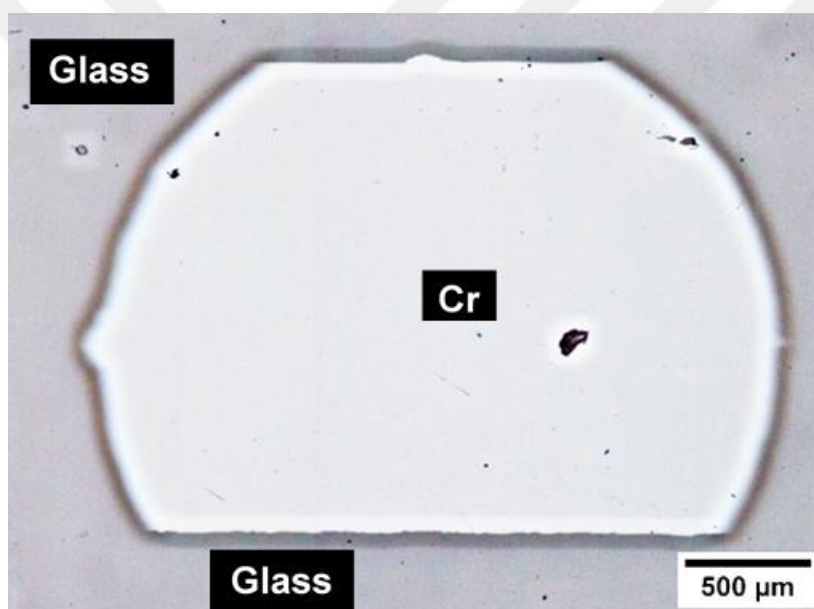


Figure 3.2 : Shows chromium thin film on glass. Bright area that distinguished from rest is thin chromium film.

As deposition finished we left samples in the vacuum chamber and pulled out on the next days. We carefully removed kapton tape and took out from mask using tweezers. It is very important to handle chromium thin film sample carefully.

3.2 Graphene Transferring

After thin film chromium deposition, CVD-grown graphene is transferred onto Cr/glass. After that gr/Cr/glass sample was put in a petri dish and was filled with acetone and heated at 55°C for an hour. Then gr/cr/glass immersed into IPA for 30

minutes. At the last stage 30 minutes with DI water. Fishing graphene on chromium thin film on glass is difficult. Some area of graphene is torn because we dry with nitrogen gun and indicated in figure 3.3.

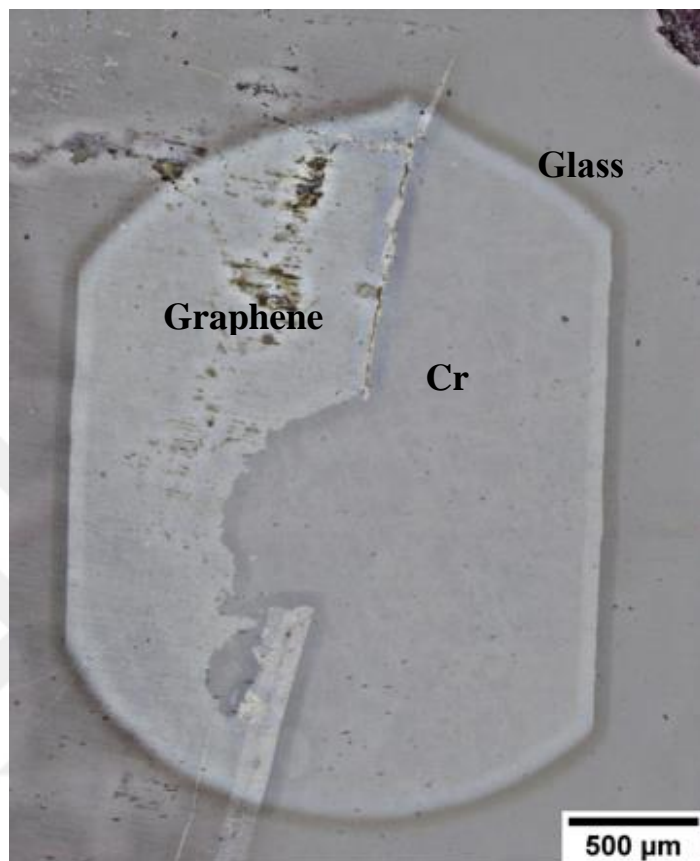


Figure 3.3 : Description of graphene/chromium/glass system.

3.3 Annealing and Production of Cr_xO_y particles

Samples were annealed in a tube furnace at 450°C for approximately 20 minutes. We used an extra thermocouple for temperature reading. Reference thermocouple was main for time count down, as we inserted the sample into the tube furnace and waited until reading external thermocouple reached 450°C. As the temperature reached 450°C, countdown started and the sample stayed in the tube furnace at the ambient condition without gas flow. The total exposure time to heat was 40 minutes. After conducting several processes, temperature deviation between reference and furnace thermocouple was arranged in a table. Utilizing this table, the line graph of the process was created and was depicted in the figure 3.4 B.

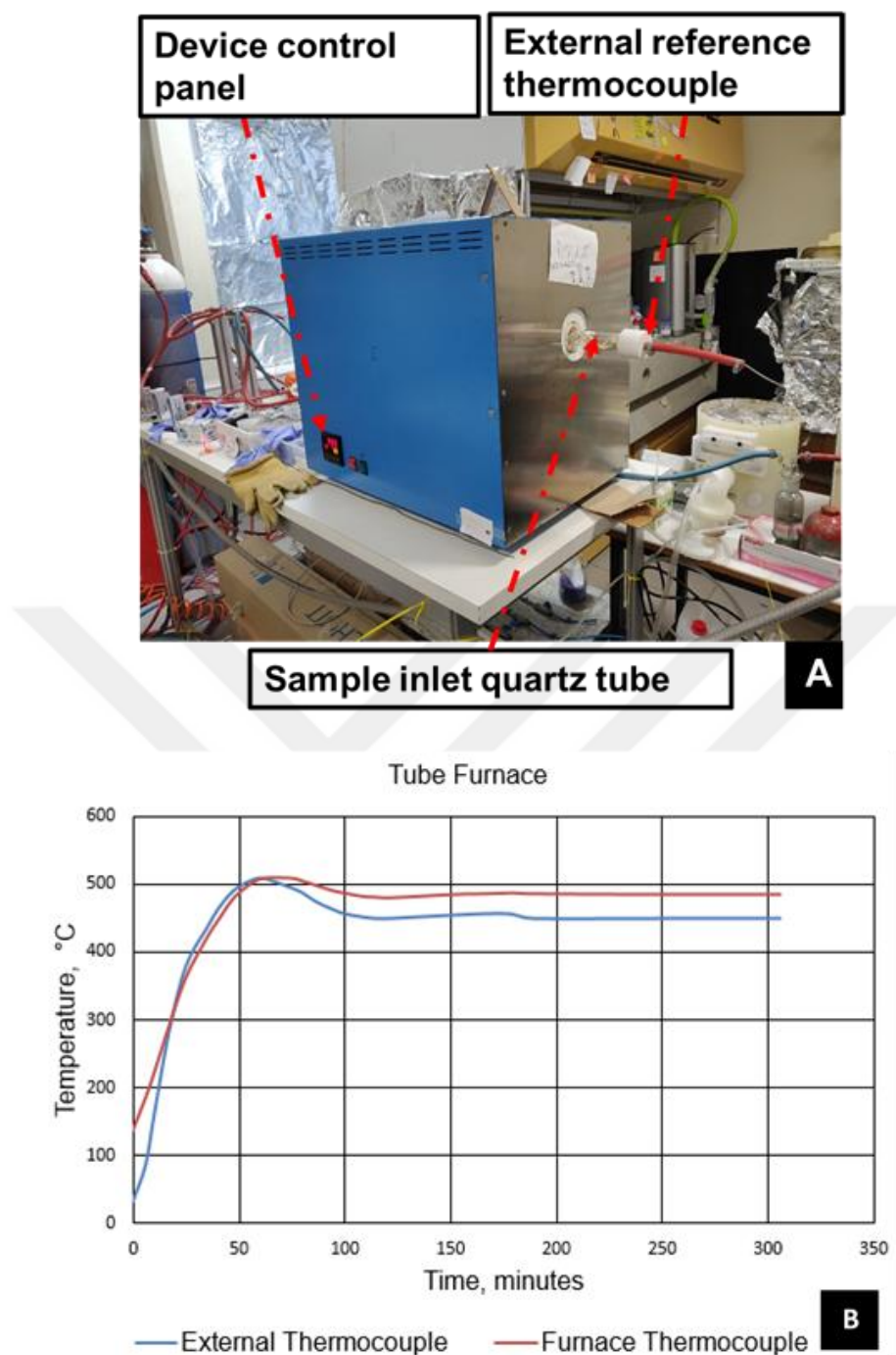


Figure 3.4 : CVD furnace, A-tube furnace view, B-graph of heating rate and temperature stabilization.

Figure 3.5 indicates annealed chromium thin film on glass. Heat produced chromium oxide nano particles. We use ImageJ so as to count particle size. Procedure was as follow we convert data to binary data, in order to distinguish particle better watershed is used, scale bar is set and particle size is analysed. Average particle size in figure 3.5 c) is $0.555\mu\text{m}$.

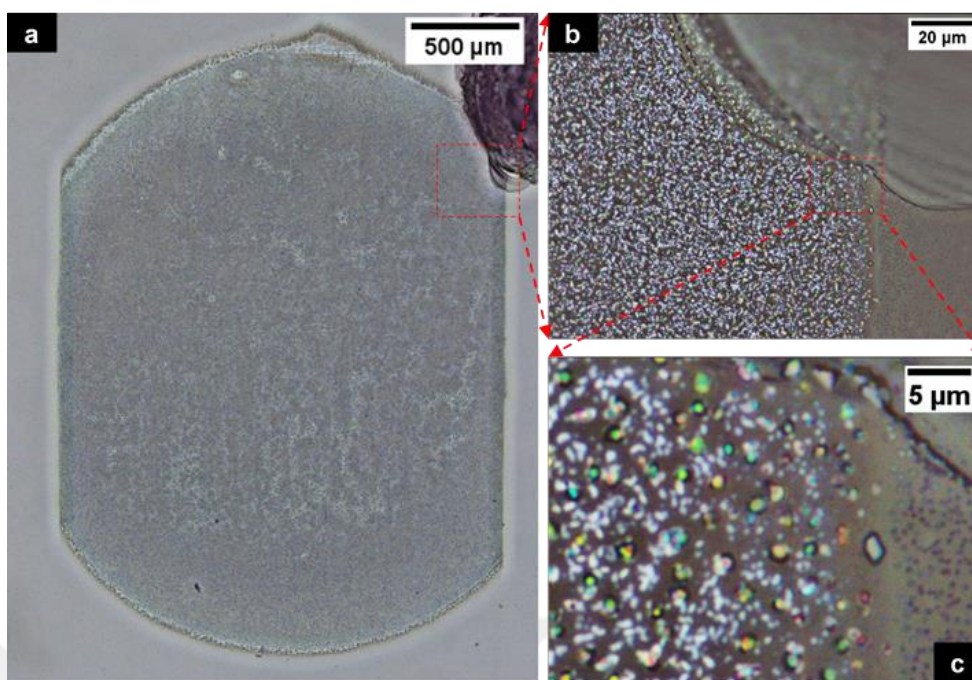


Figure 3.5 : a)-Depicts $\text{Cr}_x\text{O}_y/\text{glass}$ after 450°C at $500\mu\text{m}$, b)-depicts inset of $\text{Cr}_x\text{O}_y/\text{Glass}$ at $20\mu\text{m}$, c)-shows $\text{Cr}_x\text{O}_y/\text{Glass}$ at $5\mu\text{m}$. Bright spots are chromium oxide nanoparticles.

Figure 3.6 shows Graphene/ $\text{Cr}_x\text{O}_y/\text{glass}$ after annealing at 450°C for 20 minutes (total time 40 minutes).

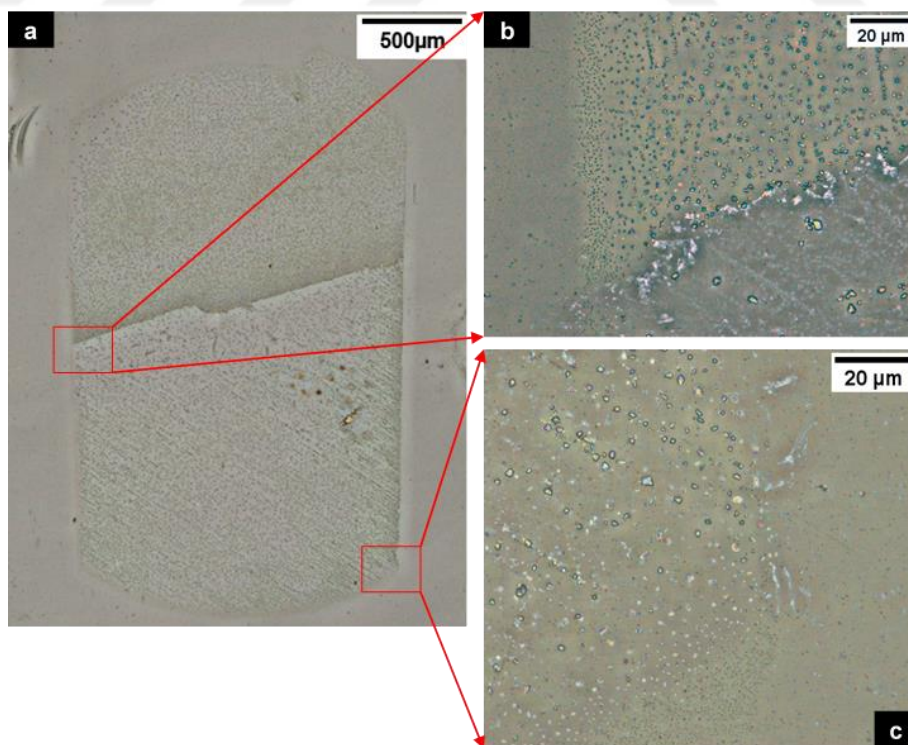


Figure 3.6 : a)-Grpahene/ $\text{Cr}_x\text{O}_y/\text{Glass}$ after annealing at 450°C at $500\mu\text{m}$. Inset from b-indicates graphene/ $\text{Cr}_x\text{O}_y/\text{glass}$ edge. Inset from c-indicates graphene/ $\text{Cr}_x\text{O}_y/\text{glass}$ from lower right.

As it went through heat treatment we retrieved it and observed under optical microscope before controlled humidification. We kept them in container filled with silica gel in order to preserve from environment humidity.

3.4 Graphene/Mica

A piece of graphene was cut from a sheet of CVD grown graphene on copper foil, then coated with Poly (methyl methacrylate) shortly PMMA using spin coating device and stored in desiccator. Next step was graphene etching under the copper foil (during CVD process, graphene grows over and under copper foil) for 3-4 minutes in nitric acid (HNO_3 , dissolve nitric acid with water in 1:3 ratio) until bubbles appeared. Next stage was to place into solution of FeCl_3 to etch the copper foil and left PMMA supported graphene. After 3 hours in solution, it is washed with DI water 3 times and fished onto substrate. Cleavage process conducted utilizing scotch tape before transferring graphene onto mica. Figure 3.7 illustrates basic graphene mica system.

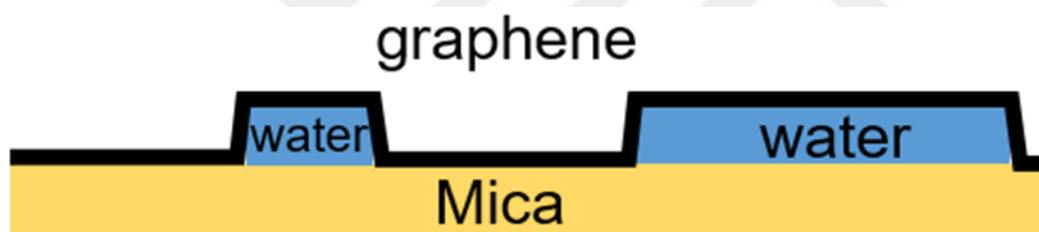


Figure 3.7 : Basic illustration of graphene on mica. Pale yellow is mica substrate, blue one is intercalated water and black one over mica and water is graphene sheet.

3.5 Water Interaction/Deposition on Cr_xO_y /Glass

Isolation box was made from transparent stretch film. Firstly, we put aluminum foil under the optical microscope with dimension approximately 57cmx66cm. Then using Thorlabs mounting post and aluminum profiles made scaffold. As soon as frame was ready we enclosed optical microscope with stretch film and scotch tape. Silica gel container was put into stretch box so as to dry and maintain dryness. After some period of time, silica gel is required to renew. Dry silica gel is blue colour. Purple and orange colour indicate that silica gel is hydrated. By heating at 120°C - 130°C we regenerate silica gel (turn blue color). By this method humidity within stretch box reduced as minimum as 9%. To preserve stretch box to catch humidity from outside I used polyethelene plastic bag and use them as a glove. By doing that it is possible to

maintain constant dryness inside, while depending on a season humidity fluctuates. Controlled humidification conducted with nitrogen gas cylinder, bubbler and flowmeter. On purple background is nozzle. We used plastic pipette tip as a nozzle and held it with hand. Whole set up illustrated at below in figure 3.8. Nitrogen from gas cylinder flow through flowmeter adjusted to 80-100 sccm flow rate. Then dry nitrogen gas enter bubbler and left as humidified. In figure 3.8 set up for controlled humidification is described.

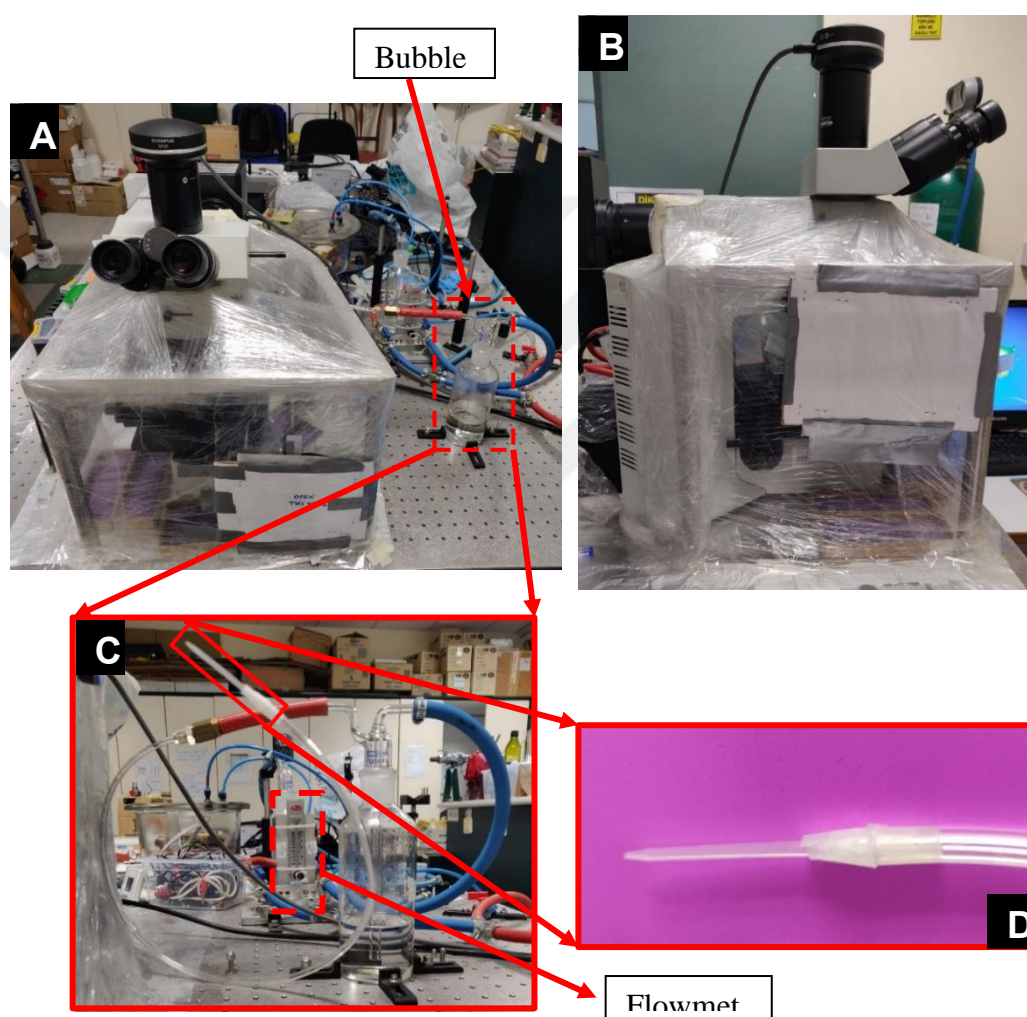


Figure 3.8 : Optical microscope enclosed with stretch film and humidification unit. A-front view, B-side view, C-bubbler and flowmeter, D-nozzle.



4. RESULT AND DISCUSSION

4.1 Comparison of Fractal Formation Related to Deposited Thin Cr Film and Deposition Time

We kept sample preparation parameters constant except the chromium deposition time. We changed only the one parameter, deposition time (thickness). Later we convert it to the thickness. Samples are exposed approximately to 95A current for various times. Annealing process at the early stage was total 20 minutes and this was not enough for producing chromium oxide nano particles. Figure 4.1 shows lack of the the heat treatment. Some areas left intact after the heat treatment, so we decided to start count down from reference thermocouple reading. In this condition total heat treatment rised to 40 minutes. Figure 4.2 shows in sequential deposited, annealed and fractal formation of 16 nm chromium thin layer on glass. Drying process after humidification led to the formation of fractal structures at the fringes of the sample.

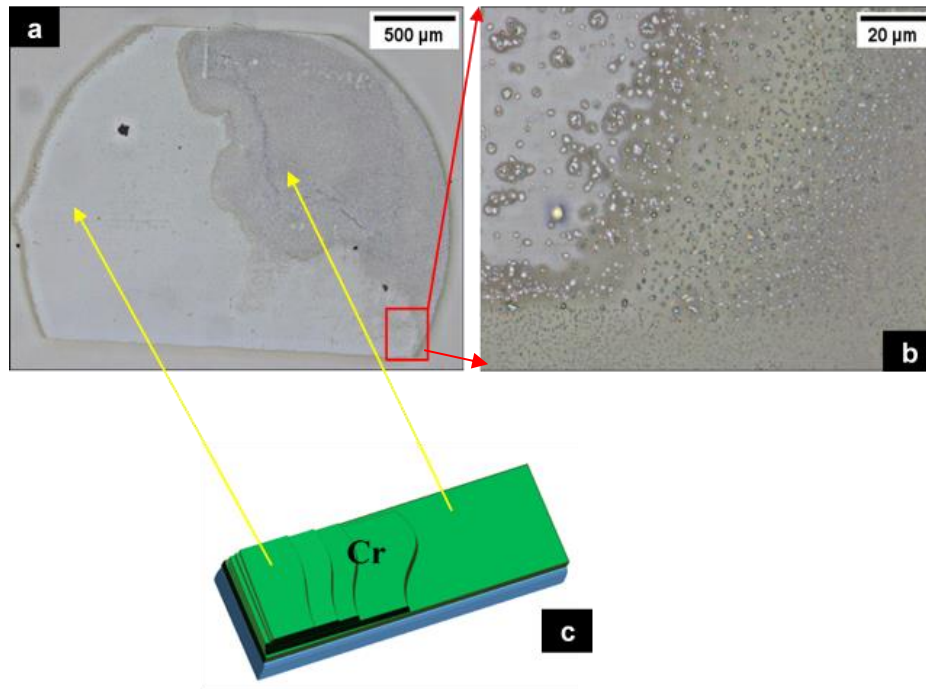


Figure 4.1 : Pictures show chromium thin film sample that did not annealed homogeneously. a) shows sample with 500μm scale bar. b) Shows sample at 20 μm scale bar. c) explain chromium thickness distribution on sample (green-chromium, blue-glass substrate).

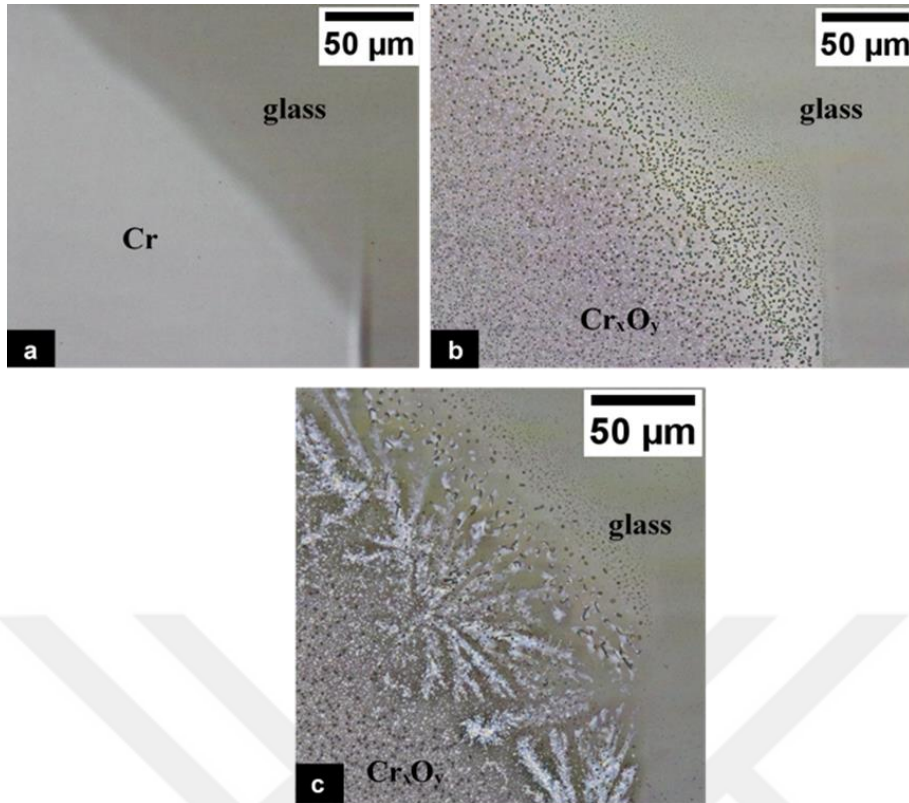


Figure 4.2 : Indicated optic data was taken from exactly same location of the sample. Scale bar is 50μm. a is after thin film cr deposition, b after annealing at 450°C, c after first controlled humidification.

We compare samples produced by Kivanc [2] with our samples and observed differences. The most significant causes for such indicator were that our samples annealed at 450°C. Kivanc Esat did annealing at 500°C for 20 minutes. In Kivanc case thickness of samples were constantly 10 nm chromium thin film. In our case thickness of the deposited chromium is varied. We did color correction and color balance to better detect thin film chromium. Figure 4.3 indicate thin film chromium on glass at 200 μm scale bar. In figure 4.3 c and d are our samples before annealing and after annealing. In d part color correction made it visible.

Our sample thickness illustrated in figure 4.3 c) is 12 nm. In figure 4.3 d, despite the fact that color correction made edge of chromium thin layer distinguishable, it was still hard to observe it with naked eye.

Figure 4.4 shows comparison Kivanc and our samples chromium oxide nano-particles at 10μm scale bar. In both we can detect chromium oxide nano particles. In our case chromium nano oxides are distributed as scattered and did not form nano oxide cluster. We did not observe fractal from water interaction on the whole surface of the sample. Our samples showed locally fractal formation.

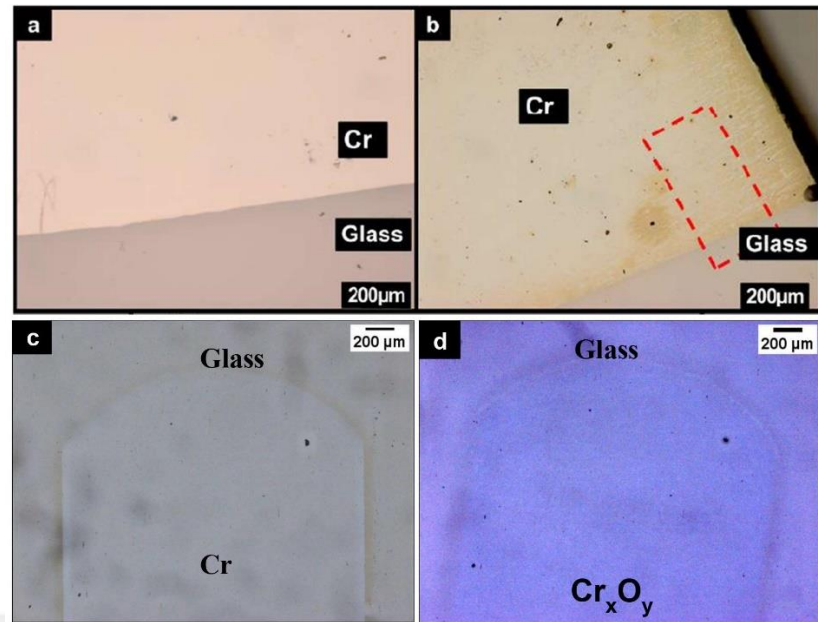


Figure 4.3 : Comparison of thin chromium film before and after annealing. a- after chromium deposition, b-after annealed at 500°C, c-after deposition, d- after annealed at 450°C.

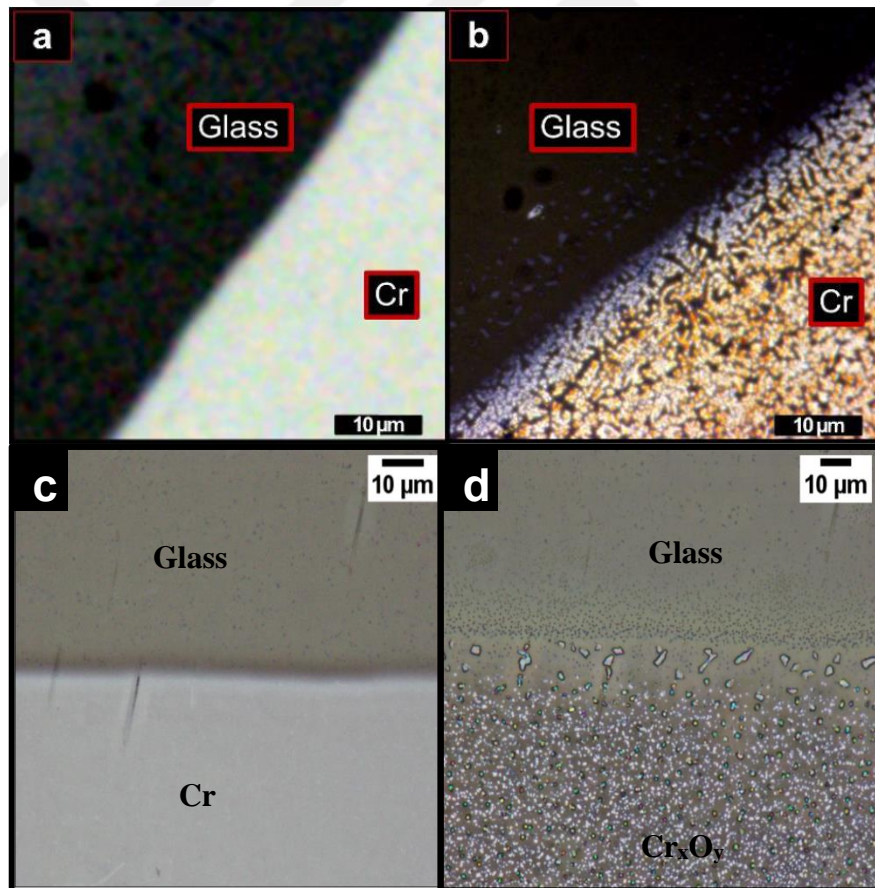


Figure 4.4 : a and b give information about samples produced by Kivanc Esat a)chromium ultra thin film on glass and b) chromium oxides nano particles on glass. c and d our samples. c) after deposition of thin film chromium on glass and d) chromium oxide nanoparticles on glass.

25 nm thin film chromium was deposited on soda lime glass. In figure 4.5 a) photo showed chromium on glass deposition and the thickness of thin film chromium is less at the fringe of the sample. After annealed at 450°C for approximately 40 minutes. In b) heat treatment created chromium oxides nano particles. We humidified it in controlled manner. In c) showed picture with water droplets on chromium oxide thin film. As it dried we could not observe clear and neat fractal formation. Picture d) showed after water droplets dried.

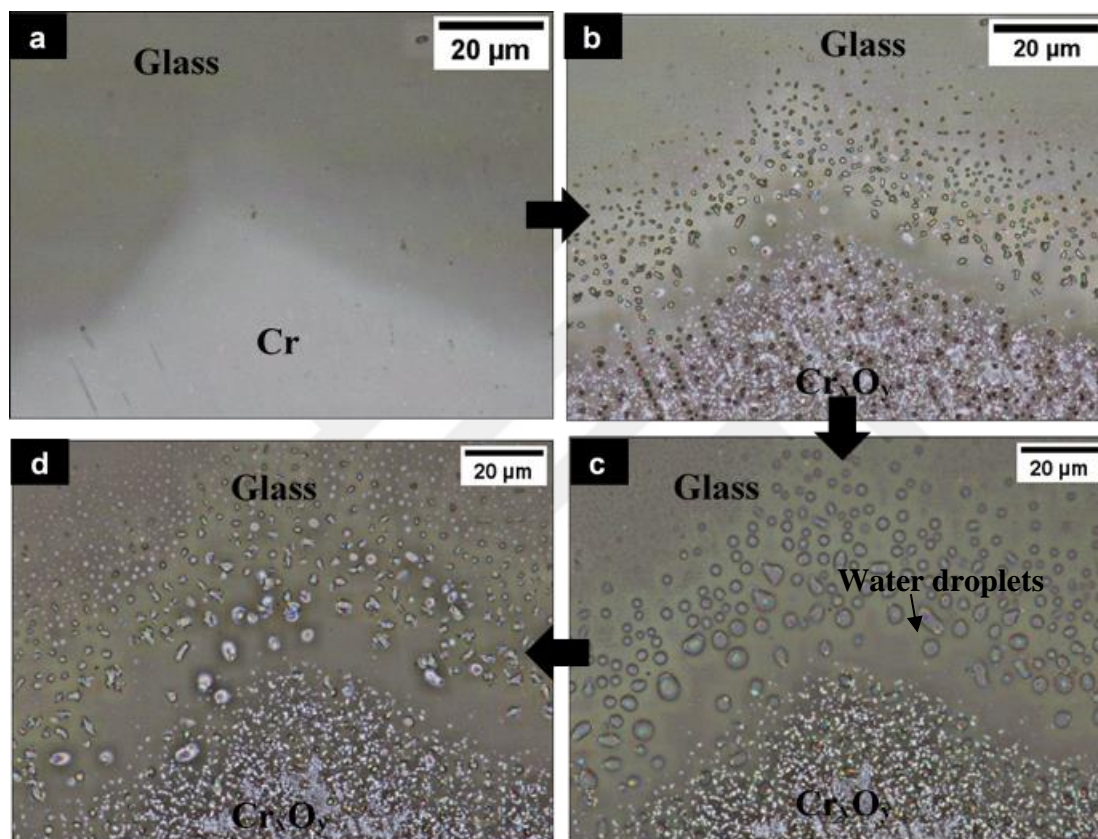


Figure 4.5 : Illustration chromium thin film on glass, a after deposition, b-after heat treatment at 450°C, c-during humidification, d-after humidification.

4.2 Water Interaction With Graphene/Cr_xO_y/Glass

Glass substrates cut from microscope slide dimension 5mm by 5mm. Reference mark was made on all substrate in order to distinguish deposited face of substrate. Chemical cleaning was done in ultrasonic bath with acetone, IPA, methyl alcohol and DI water each of them respectively 5 minutes. Accidentally, we missed methanol cleaning step in preparation process of this sample. Chemical cleaning was repeated second time with full step. Then dried with nitrogen blow and expose to plasma cleaning with argon (45sccm) and oxygen (5sccm) gas mixture for 5 minutes. As substrates cleaned they

were put into mask and fixed with Kapton tape. Deposition process was done on 12.03.2021. Deposition parameters were the followings: current 95-96 A, pressure in vacuum chamber 7.42×10^{-6} mbar, thickness of deposited chromium thin film was approximately 12 nm (deposition time 180, at that times we did not use thickness monitor). Samples stayed in vacuum chamber over night and taken out next day. On 29.06.2021 graphene was transfered onto chromium thin film glass substrate and next day was exposed to 450°C for 20 minutes (count down started from external thermocouple reading) and total duration of staying sample in tube furnace was approximately 40 minutes. On the following day sample were observed with optical microscope. Plastic bag was used in order to preserve inner part of dry box from enviroment humidity and manipulate polyethelene. Plastic bag was functional and it served as cheap gloves. We blow with humid nitrogen for 5 minutes and the humidity within box rised to 41%. To maintain at the same location was difficult. That's why we did not do more than 5 minutes. In figure 4.6 consecutively described sample condition.

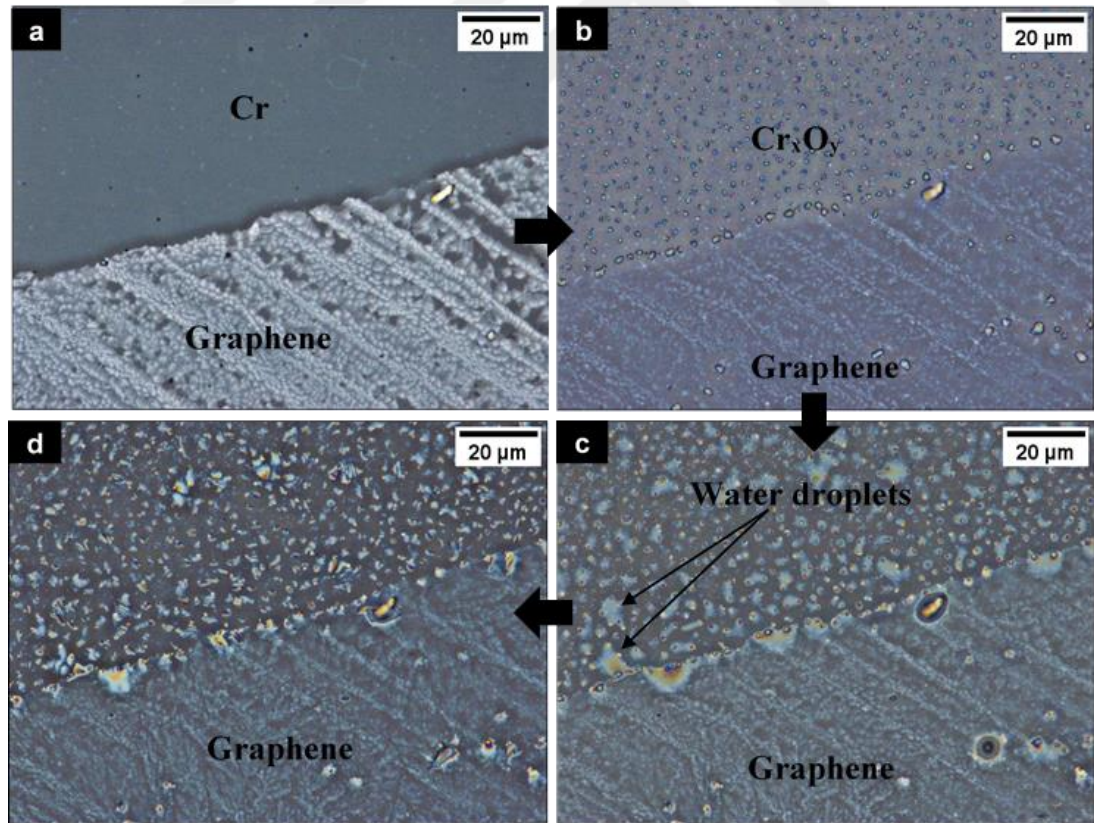


Figure 4.6 : Graphene/ Cr_xO_y /Glass system.

We observed fractal formation at different locations. Figure 4.7 depicts fractal formation on two sides of the sample: on both Cr_xO_y /glass and graphene/ Cr_xO_y /glass

sides. All photos in 4.7 were color corrected. Fractals on non-graphene part has thinner branches. They nucleated and extended from one point, as this point is seed point. Figure 4.7 b shows fractals on non graphene part. On graphene part fractal formed as flower and branches are thicker.

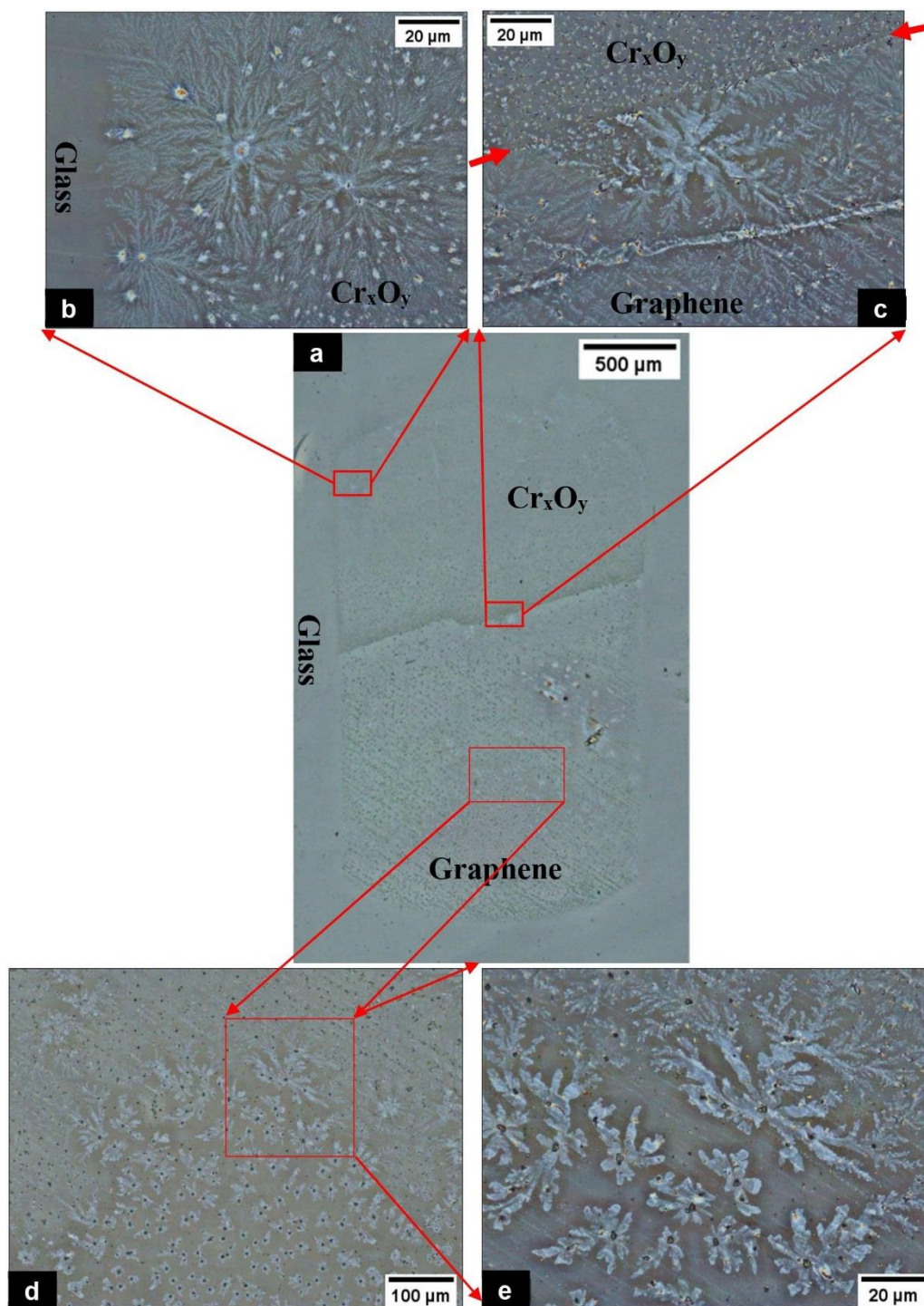


Figure 4.7 : a-graphene/chromium oxide nano particle,b-fractal formed at non-graphene side of sample surface after humidification,c-fractal at chromium oxide nano particle graphene edge(red arrows in c indicate graphene frontier) d-inset indicate fractals at 100μm scale bar and e-indicate fractals at 20μm scale bar.

As previous samples in this sample fractals distributed unevenly. Figure c, d and e illustrate fractal formed on graphene part of sample. We prepared another sample with same parametrs except thickness. CVD grown graphene is transfered onto 19 nm thin chromium film and annealed at 450C for total 40 minutes. In figure 4.8 there is shown graphene/CrxOy/glass sample.

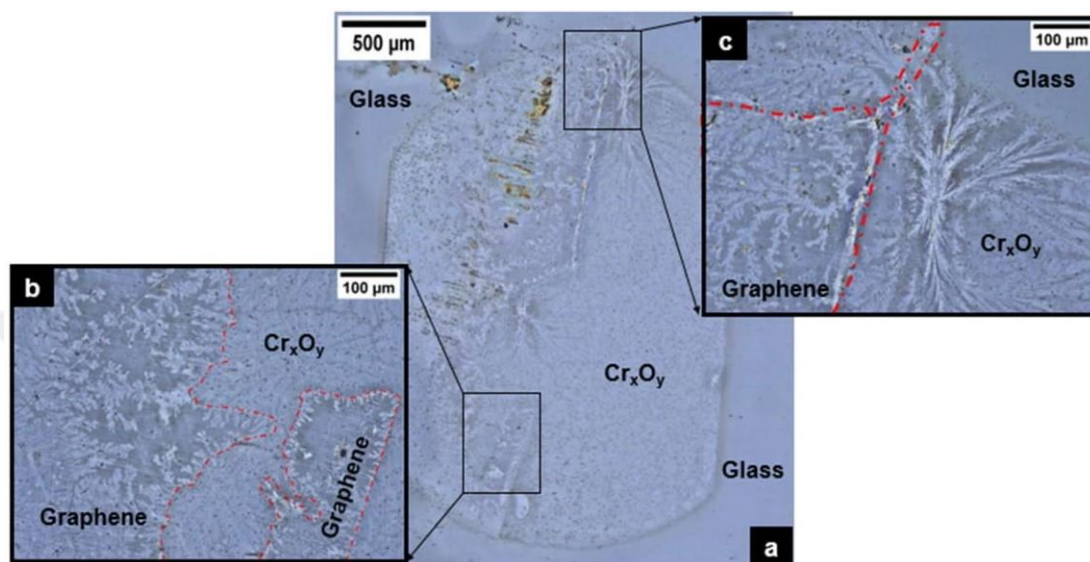


Figure 4.8 : a) graphene/CrxOy/glass at 500μm scale bar. b) red dotted enclosed lines shows graphene area, rest shows Cr_xO_y area, c) red dotted line indicates graphene covered area, rest area Cr_xO_y and glass.

We did color correction with ImageJ to see details.

4.3 Comparison of Surface Fractal formation on Graphene/Mica Samples

4.3.1 Rewetting in isolated box

We tried to reduce humidity in dry box and for this purpose silica gel is used. Stretch box filled with container that contain dry silica gel (blue colour). By this manner it was possible to reduce humidity 9% but at the morning humidity was 20% due to morning dew point. We connect dry nitrogen tube using pneumatic tube to stretch box and adjust less than 2 bar pressure by reducer. By this method humidity within dry box reduced to 4.5% then we made attempts to observer de/rewetting at interface of graphene/mica. We left sample overnight to equilibrium with dry box atmosphere. Unfortunately, next day in the morning humidity was 20%. Overnight waiting in stretch box didn't work.

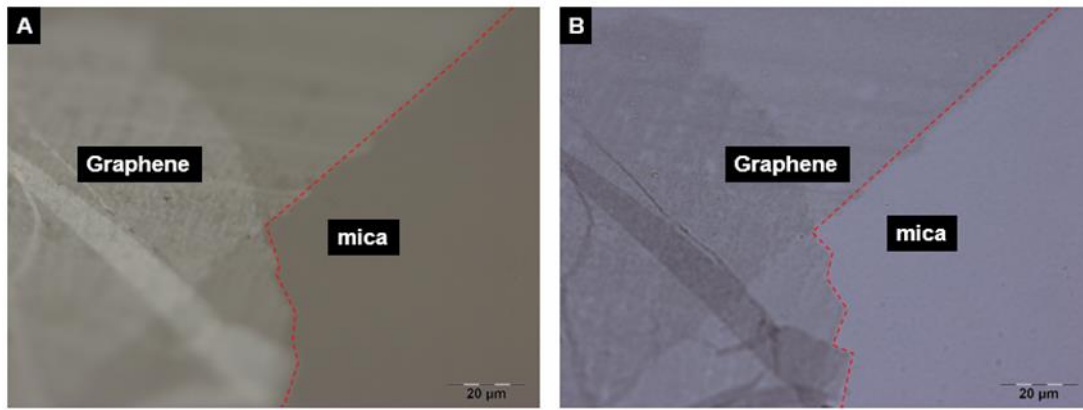


Figure 4.9 : Graphene/Mica. A describes direct illumination Optic data, B describes back reflected illumination Optic data.

4.3.2 Rewetting with graphene heater

For this purpose Stamping set up is utilized and graphene heater is produced. Graphene heater allows us to heat up to 200°C. We tried several times nevertheless faced with fault owing to lack of resolution and lighting make it difficult to observe.

5. CONCLUSIONS

In this master thesis, our goal was observation and investigation of the structure of water that interacts with graphene/CrxOy/glass and graphene/mica. For this purpose, we assembled PVD (thermal evaporation system) system and enclosed an optic microscope in order to preserve the observation process from ambient humidity.

In case of graphene/CrxOy/glass we prepared series of samples with varied thicknesses of chromium. Using enclosed optical microscope samples were studied. We managed to see the fractal formation. However, they were local fractal formations. On the graphene side of the sample fractals formed, as well. Formation of fractal initiated from nucleation point. Fractal formed both on graphene and non-graphene sides of the sample. We observed directionality on transferred CVD graphene. Fractals formed on the CrxOy side have thinner branches nucleated from a point and these fractals do not intersect with other fractals branches, where fractals formed on graphene have thicker branches.

In case of graphene/mica, we had tried two methods: humid isolation and heating. Unfortunately, we could not detect water intercalation with both methods.

In the future, we are planning to investigate graphene/CrxOy/glass samples with AFM.



REFERENCES

- [1] **N. Severin, P. Lange, I.M. Sokolov, J.P. Rabe**, (2012) *Nano Lett.* 12 774–779.
- [2] **K. Esat**, 2013. *Fractal Morphology of Water on Chromium-Oxide Thin Films*, Istanbul Technical University,
- [3] **N. Gray**, (2009) *Nat. Cell Biol.* 11 S8–S8.
- [4] *Vapor Pressure Curves for Common Elements*, 2018.
- [5] **M.S. J. Hu, X.-D. Xiao, D. F. Ogletree**, (1995) *Science* (80-.). 268 267–269.
- [6] **J.R.H. Ke Xu, Peigen Cao, James R. Heath**, (2013) 329 1188–1191.
- [7] **J. Song, Q. Li, X. Wang, J. Li, S. Zhang, J. Kjems, F. Besenbacher, M. Dong**, (2014) *Nat. Commun.* 5 1–8.
- [8] **O. Ochedowski, B.K. Bussmann, M. Schleberger**, (2014). *Sci. Rep.* 4
- [9] **H. Lin, J.D. Cojal González, N. Severin, I.M. Sokolov, J.P. Rabe**, (2020) *ACS Nano* 14 11594–11604.
- [10] **P. Bampoulis, K. Sotthewes, E. Dollekamp, B. Poelsema**, (2018) *Surf. Sci. Rep.* 73 233–264.
- [11] **D. Muñoz-Santiburcio, D. Marx**, (2021). *Chem. Rev.*
- [12] **N. Jiang, J. Silcox, J.** (2000) *Appl. Phys.* 87 3768–3776.
- [13] **N. Jiang, J. Silcox**, (2000) *Mater. Res. Soc. Symp. - Proc.* 589 377–382.
- [14] **S. Weisenburger, V. Sandoghdar**, (2015) *Contemp. Phys.* 56 123–143.
- [15] **E. Meyer, H.J. Hug, Roland Bennewith**, 2004. *Scanning Probe Microscopy: The Lab on a Tip*,
- [16] **H. Spence**, 2019. *Handbook Microscopy*,
- [17] **C.J. Chen**, 2007. *Introduction to Scanning Tunneling Microscopy: Second Edition*,
- [18] **R. García, R. Pérez**, 2002. *Dynamic Atomic Force Microscopy Methods*,
- [19] **C.G. G. Binning, C.F. Quate**, (1986) *Phys. Rev. Lett.* 56 5-1-5–9.
- [20] **M. Mils**, (2018). *TAYLOR HOBSON*
- [21] **M.Z. T. Chi, T. Ballinger, R. Olds**, *Surface Texture Analysis Using Dektak Stylus Profilers*, n.d.
- [22] **D.M. Mattox**, 2009. *Deposition (PVD) Processing Second Edition Dedication To My Wife Vivienne*,
- [23] *Inficon, SQM-160, Multi-Film Rate/Thickness Monitor, Operation Manual*, 2012.
- [24] **C.S. Lu, O. Lewis, J.** (1972) *Appl. Phys.* 43 4385–4390.

- [25] **J.G. Miller, D.I. Bolef, J.** (1968) *Appl. Phys.* 39 5815–5816.
- [26] **G. Sauerbrey,** (1959) *Zeitschrift Für Phys.* 155 206–222.



APPENDICES

APPENDIXE: A

Introduction: PVD is used for evaporation/deposition materials to substrate. PVD system assembled in our lab is illustrated below.

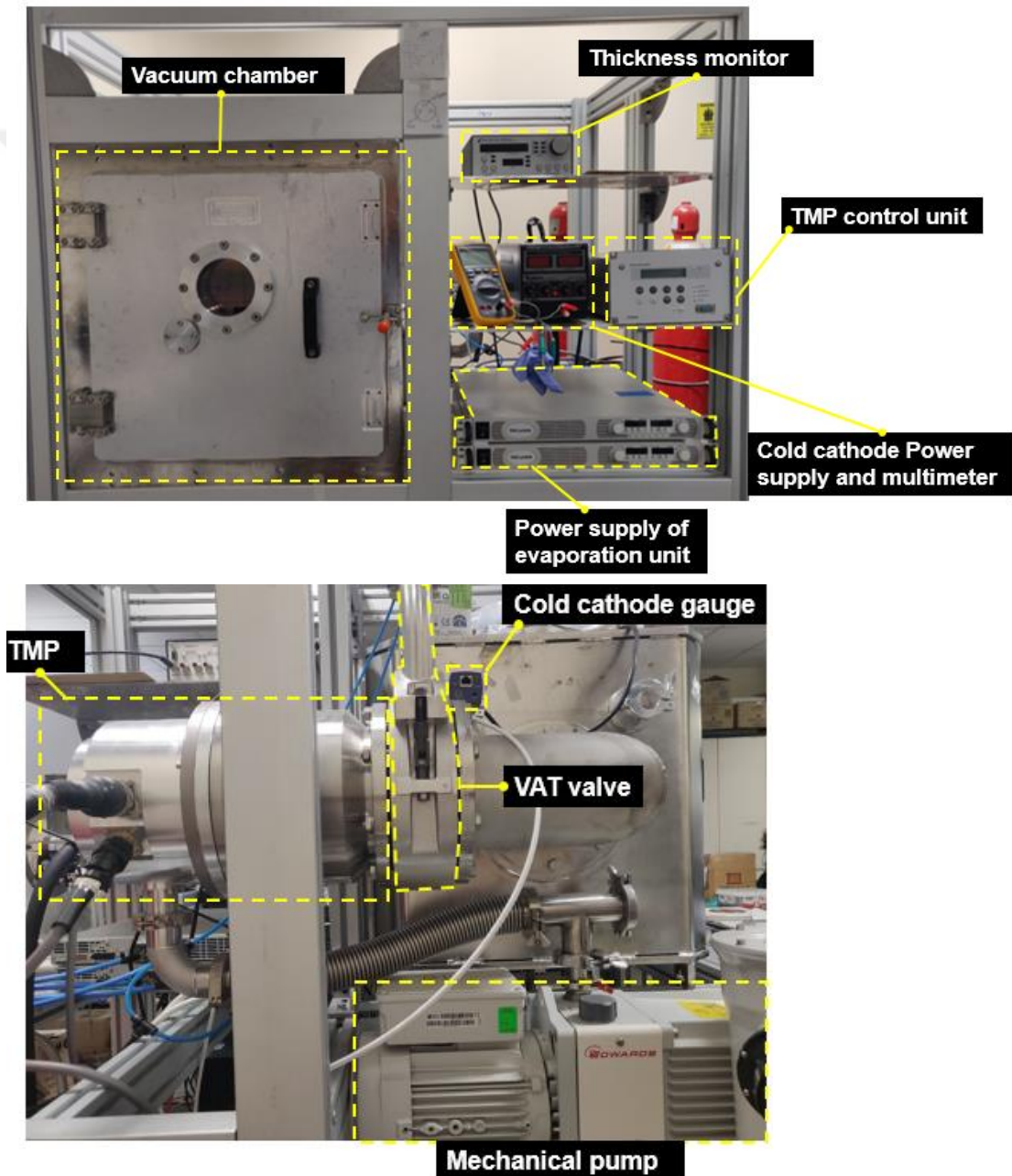


Figure A.1 : Front side and backside view of PVD system.

Pre-start preparation:

Do visual check prior to start the job. Release vacuum chamber from rear side of chamber. Loosen clamp of blind located at rear side of vacuum chamber. Slowly and carefully crack the vacuum. Open chamber door keep in mind viton sealing drop down easily, open it gently. If needs wipe viton sealing with Isopropil alcohol or methyl alcohol using tissue. Then gently apply vacuum grease and rub it gently. As soon as viton sealing is ready put it into place. Carefully locate samples into chamber and locate samples in vacuum chamber in position that it will be directly over evaporation boat. Then close the main door. Pay attention to hinge of the door. Plug in devices into power strip socket and plug in that power strip into UPS socket. Connect VAT valve pneumatic hose to nitrogen tank.(keep in mind that nitrogen tank is under high pressure) Adjust 4 bar at pressure regulator (4-7bar needs for VAT valve operation) and place VAT valve in open position. Registry every action in detail in log book and e-log book (excel sheet).

Operation Procedure:

1. Turn on Rough vacuum pump (Pump down during 20-30 minutes, after indicated period of time use MPG500)
2. Turn on vacuum gauge(MPG500)(plug Ethernet cable in vacuum gauge)



Figure A.2 : Connection order of vacuum gauge to power supply and multimeter.

Connect solid green to positive terminal and green white striped to negative terminal of power supply. Brown white stripe to com port and white orange to another port.voltage should be 14.5V and current 0.07A

3. Turn on TMP (as pressure decrease to 10^{-3} mbar)
4. Open cooling system (Cool down QCM and evaporation unit)

5. Turn on thickness monitoring (SQM160) (frequency of the crystal will oscillate then stabilized)



Figure A.3 : SQM160 thickness monitor.

There are 2 menu: Film menu and System menu

Film menu

- Press Prog. → scroll knob to film 3 and press knob → press Next or Prev for moving along parameters → adjust value by scrolling knob → press knob or next to save changes → press Prog to exit film menu (Density, Z-ratio and Tooling must be entered)

System menu

- Prog → Prev → scroll knob and select Display → select one of 4 parameters: THCK(Å), THCK(NM), Mass and Frequency → press Prog. To exit system menu (in case of nm thickness will be indicated as $0.0239\mu\text{M}=23.9\text{nm}$)

For deposited materials parameters see below table. We generally use Chromium, Copper and Gold. Table A.1 shows materials name and their parameters.

Table A.1 : Material table.

Formula	Density	Z-Ratio	Material Name
Au	19.300	0.381	Gold
Cr	7.200	0.305	Chromium
Cu	8.930	0.437	Copper

6. Turn on evaporation unit power supply (start deposition as pressure decrease to $A \times 10^{-6}$ mbar (A-any number)).



Figure A.4 : Evaporation unit power supply.

Switch on power supply and press out button then using both knobs adjust current to the desired value. During deposition/evaporation process take multimeter, thickness monitoring and if desired temperature with thermocouple mounted on to evaporation unit. Be careful electrical shock it can heavily injure or cause death. [Power supply photo has taken from e-bay.com].

Closing Procedure:

Scroll power supply knob until value at display reached zero. Then press out button and turn off it after 10-15 minutes. After that press brake button on TMP control panel. As soon as brake button pressed during 5 minutes revolution drop down from 100% to 0%. At 20% rotation close VAT valve (close open position and open close position) turn off rough vacuum pump. Close cooling system. Switch off thickness monitoring. Disconnect pneumatic hose from nitrogen tank.

Schematic diagram of PVD showed in figure A.5.

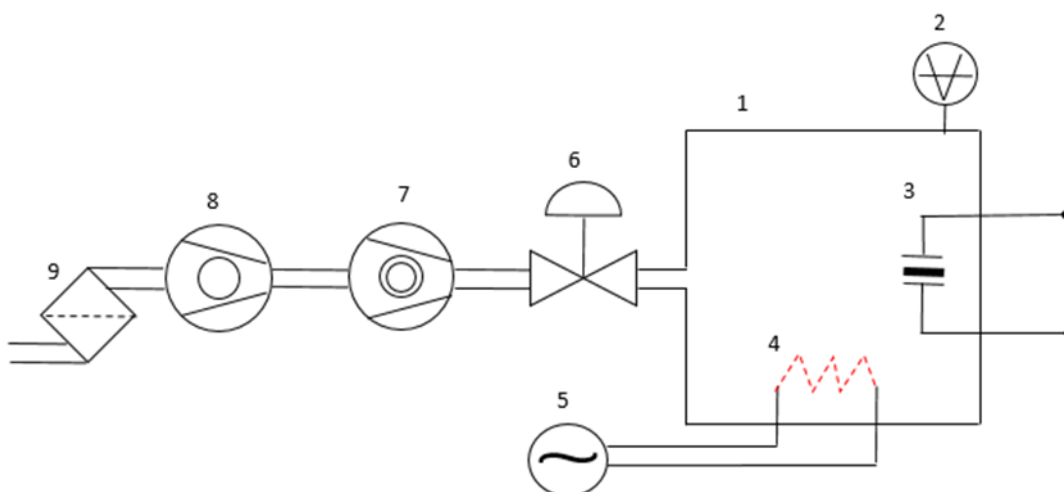


Figure A.5 : P&ID of PVD system. 1 vacuum chamber, 2 vacuum gauge, 3 Quartz Crystal Microbalance, 4 Evaporation unit and Mo boat, 5 power supply, 6 VAT (pneumatic) valve, 7 TMP, 8 Rotary positive displacement pump, 9 mist filter.

APPENDIX: B

QCM calibration

To calibrate QCM and identify tooling factor we produce 3 set of samples. Each set contained 3 Si wafer and chromium deposited on them. Si wafer has smoother surface and this gives opportunity to identify thickness of deposited material more accurately. For this reason we used Si wafer. At the first deposition SQM160 reading was 13.5 nm, in second reading was 20.5 nm and in the third deposition it showed 23.9 nm thickness. Origin Lab is used to create graphic. The measurement of the samples are done with Bruker DEKTAKTX profilometer.

Figure B.1 shows sampling location and respective graph of the profile reconstructed in OriginLab.

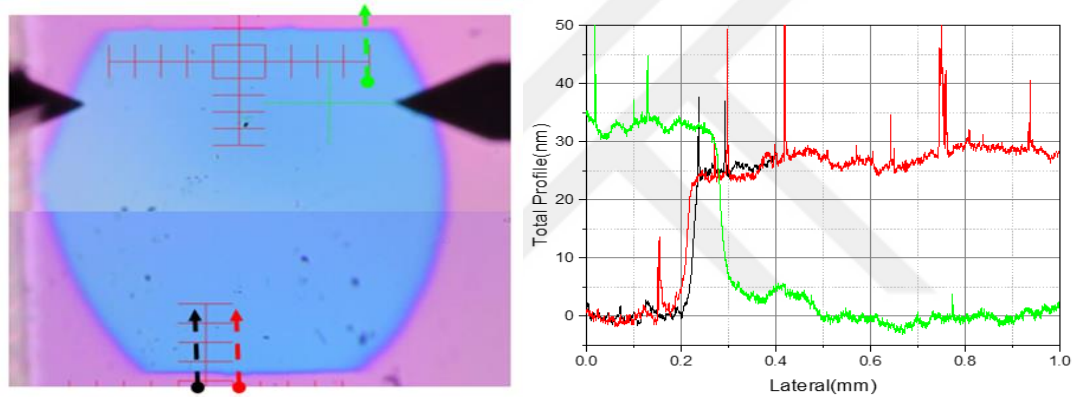


Figure B.1 : 13.5 nm thin film chromium on Si wafer. Red, green and black arrows indicates profilometer stylus movement direction.

We marked profilometer stylus scanning direction with colored arrows. Figure B.2 illustrates second set of samples that have 20.5 nm thickness.

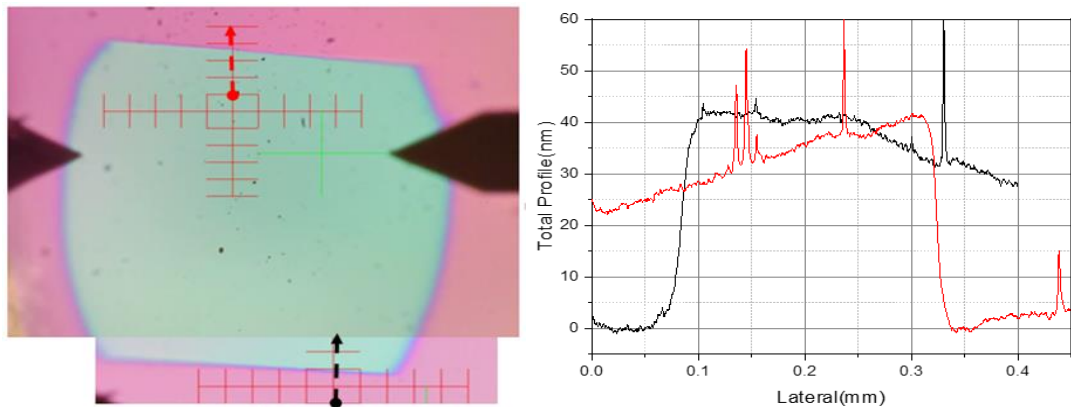


Figure B.2 : 20.5 nm thin film chromium on Si wafer. Red and black arrows indicates profilometer stylus movement direction.

Figure B.3 shows third set of deposited Si wafers with 23.9 nm thickness.

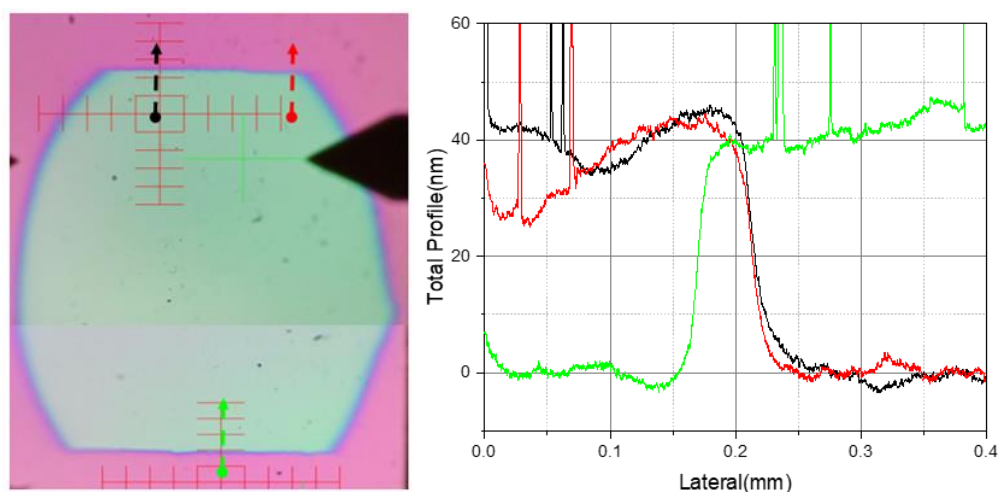


Figure B.3 : 23.9 nm thin film chromium on Si wafer. Red, green and black arrows indicates profilometer stylus movement direction.

Third deposition thickness was 23.9 nm according SQM160 and illustrated below.

We calculate the thickness of deposition according the thickness monitor reading and profilometer measurement. First and third set showed similar correlation. Second deposition thickness is slightly different. Taking into consideration we compose table and calculate tooling.

Table B.2 shows calibration value of the QCM

Table B.1 : QCM calibration table.

Process#	Actual measured average thickness, nm	Device Reading, nm	Average Tooling, %
1	26.62	13.5	
2	35.26	20.5	188%
3	46.84	23.9	

According calculation tooling for SQM160 is 188%.

CURRICULUM VITAE

Name Surname : Orkhan NOVRUZOV

EDUCATION :

- **B.Sc.** : 2008, Baku State University, Chemistry, Department
- **M.Sc.** : 2013, Azerbaijan State university of Oil and Industry University, Chemical Technology, Synthesis of organic substance and Industrial ecology